

63-3-2

ASD-TDR-62-1086

401 810

CATALOGED BY ASTIA
AS AD No. 401810

**RESEARCH ON GROWTH AND DEFORMATION MECHANISMS
IN SINGLE CRYSTAL SPINEL**

TECHNICAL DOCUMENTARY REPORT NO. ASD-TDR-62-1086

February 1963

Directorate of Materials and Processes
Aeronautical Systems Division
Air Force Systems Command
Wright-Patterson Air Force Base, Ohio

Project No. 1 (8-7350), Task No. 73500



(Prepared under Contract No. AF33(616)-7820
by North Carolina State College;
Hayne Palmour, III, W. Wurth Kriegel, R. Douglas McBrayer, authors)

NOTICES

When Government drawings, specifications, or other data are used for any purpose other than in connection with a definitely related Government procurement operation, the United States Government thereby incurs no responsibility nor any obligation whatsoever; and the fact that the Government may have formulated, furnished, or in any way supplied the said drawings, specifications, or other data, is not to be regarded by implication or otherwise as in any manner licensing the holder or any other person or corporation, or conveying any rights or permission to manufacture, use, or sell any patented invention that may in any way be related thereto.

Qualified requesters may obtain copies of this report from the Armed Services Technical Information Agency, (ASTIA), Arlington Hall Station, Arlington 12, Virginia.

This report has been released to the Office of Technical Services, U.S. Department of Commerce, Washington 25, D.C., in stock quantities for sale to the general public.

Copies of this report should not be returned to the Aeronautical Systems Division unless return is required by security considerations, contractual obligations, or notice on a specific document.

<p>Aeronautical Systems Division, Dir/Materials and Processes, Metals and Ceramics Lab., Wright-Patterson AFB, Ohio.</p> <p>Rpt AF ASD-TDR-62-1086, RESEARCH ON GROWTH AND DEFORMATION MECHANISMS IN SINGLE CRYSTAL SPINEL. Final report, Feb 63, 72 p., incl illus & refs.</p> <p>Unclassified report</p> <p>The first phases of a continuing program of research on growth and deformation processes in magnesium aluminate spinel are described. Spinel forming reactions, structure and properties of spinel, synthesis of spinel feed materials (including a study of the effects</p> <p>(over)</p>	<p>1. Single Crystal Spinel</p> <p>I. AFSC Project 1(8-7350 Task 73500</p> <p>II. Contract AF 33(616)-7820</p> <p>III. North Carolina State College, Raleigh, N. C.</p> <p>IV. Hayne Palmour, et al</p> <p>V. Avail fr OTS</p> <p>VI. In ASTIA collection</p>	<p>Aeronautical Systems Division, Dir/Materials and Processes, Metals and Ceramics Lab., Wright-Patterson AFB, Ohio.</p> <p>Rpt AF ASD-TDR-62-1086, RESEARCH ON GROWTH AND DEFORMATION MECHANISMS IN SINGLE CRYSTAL SPINEL. Final report, Feb 63, 72 p., incl illus & refs.</p> <p>Unclassified report</p> <p>The first phases of a continuing program of research on growth and deformation processes in magnesium aluminate spinel are described. Spinel forming reactions, structure and properties of spinel, synthesis of spinel feed materials (including a study of the effects</p> <p>(over)</p>	<p>1. Single Crystal Spinel</p> <p>I. AFSC Project 1(8-7350 Task 73500</p> <p>II. Contract AF 33(616)-7820</p> <p>III. North Carolina State College, Raleigh, N. C.</p> <p>IV. Hayne Palmour, et al</p> <p>V. Avail fr OTS</p> <p>VI. In ASTIA collection</p>
<p>of irradiation on spinel formation), techniques and apparatus for crystal growth with Verneuil oxyhydrogen and RF plasma devices, and the effect of atmosphere on precipitation hardening of alumina-rich spinel have been studied. The report includes a summary of structural and physical properties of $MgAl_2O_4$ spinel.</p>		<p>of irradiation on spinel formation), techniques and apparatus for crystal growth with Verneuil oxyhydrogen and RF plasma devices, and the effect of atmosphere on precipitation hardening of alumina-rich spinel have been studied. The report includes a summary of structural and physical properties of $MgAl_2O_4$ spinel.</p>	

FOREWORD

This report was prepared by the Department of Engineering Research, North Carolina State College, under USAF Contract No. AF 33(616) 7820. This contract was originated under Project No. 1 (8-7350), Task No. 73500. The work was administered under the direction of the Directorate of Materials and Processes, Deputy Commander/Technology, Aeronautical Systems Division, with Mr. J. B. Blandford, Jr. acting as project engineer. This report covers work conducted from February 1961 through July 1962.

The authors gratefully acknowledge the combined talents, interests, and efforts of their several co-workers; without them this report and the research it describes could not have come into being. Those directly participating in this program have included: L. D. Barnes, D. M. Choi, G. A. Hofer, and P. K. Mehta, graduate research assistants; and J. O. Barker, Jr., H. Z. Dokusogus, G. F. Hill, J. H. Scoggins, D. R. Smith, R. L. Ward, H. F. Williams, and D. E. Witter, student assistants. W. J. Lackey, Jr. and G. V. Sidler, graduate students, working in cooperation with project personnel, initiated and carried out as a class project the first phases of the study of irradiation effects on spinel formation described in Section V. The typing of the manuscript (in drafts and in final form) was entrusted to Mrs. Marion S. Rand.

The faculty and staff of North Carolina State College have generously contributed many ideas and physical resources in support of this effort. In particular, N. W. Conner, Director of Engineering Research, has provided valuable advice and counsel and much direct assistance in administrative matters; Dr. W. C. Hackler, Dr. G. G. Long, Dr. A. E. Lucier, Professor J. F. Seely, Dr. H. H. Stadelmaier, and Dr. R. F. Stoops have made special analytical or processing facilities available; and K. R. Brose and W. E. Griffin have been most helpful in acquiring and/or constructing the various items of new equipment required in this program.

ABSTRACT

PALMOUR, HAYNE III, KRIEGEL, W. WURTH, and McBRAYER, R. DOUGLAS, Research on Growth and Deformation of Single Crystal Spinel (North Carolina State College).

The first phases of a continuing program of research on growth and deformation processes in magnesium aluminate spinel are described. Spinel forming reactions, structure and properties of spinel, synthesis of spinel feed materials (including a study of the effects of irradiation on spinel formation), techniques and apparatus for crystal growth with Verneuil oxyhydrogen and R F plasma devices, and the effect of atmosphere on precipitation hardening of alumina-rich spinel have been studied. The report includes a summary of structural and physical properties of MgAl_2O_4 spinel.

This report has been reviewed and approved.



W. G. RAMKE

Chief, Ceramics and Graphite Branch
Metals and Ceramics Laboratory
Directorate of Materials and Processes

TABLE OF CONTENTS

	PAGE
I. INTRODUCTION	1
II. SPINEL FORMING REACTIONS	3
III. STRUCTURE AND PROPERTIES OF MAGNESIUM ALUMINATE SPINEL	6
Structure of Spinel	6
Ideal Structure	6
Actual Structure	8
Dislocations in the Ideal Structure	13
Twinning	13
Alumina-rich Spinel	13
Solid Solutions in the MgO-Al ₂ O ₃ System	13
Exsolution in Nonstoichiometric Spinel	14
Mechanism of Exsolution	14
Effect of Exsolution on Mechanical Properties	16
Properties of Spinel	16
IV. SYNTHESIS OF SPINEL FEED MATERIALS	17
Mechanically Mixed Oxides	17
Coprecipitated Hydroxides	17
Pilot Production	18
V. EFFECT OF RAW MATERIAL IRRADIATION ON SPINEL FORMATION	19
Theoretical Considerations	19
Experimental Procedure	20
Experimental Findings	20
X-ray Evidence of Spinel Formation	20
Differential Thermal Analyses	25
Interpretation of Results	29
Summary	31
VI. CRYSTAL GROWTH	32
Theoretical Considerations	32
Nucleation	32
Defects	32
Effects of Impurities	33

TABLE OF CONTENTS (continued)

	PAGE
Brief History of Spinel Crystal Growth	34
The Verneuil Technique	34
Definition of the Problem	34
Original Flame-Fusion Apparatus	35
Analysis of Limitations	35
Recent Modifications of the Verneuil Method	36
Alternative Methods	37
Experimental Equipment	37
Oxyhydrogen Crystal Grower	37
R. F. Plasma Crystal Grower	41
Experimental Procedures	44
Review of Control Variables and Growth Parameters	44
Loading and Aligning	47
Lighting and Warmup	48
Initiating and Maintaining Growth	48
Quench Cooling	49
 VII. EFFECT OF ATMOSPHERE ON PRECIPITATION HARDENING IN ALUMINA-RICH SPINEL	 50
VIII. SUMMARY	53
APPENDIX A: STRUCTURE AND PHYSICAL PROPERTY DATA FOR SPINEL	54
Formal Specification of the Spinel Structure	54
Space Group	54
Atomic Positions	54
Lattice Constant	54
X-ray Diffraction	54
Physical Constants	55
Melting Point	55
Density	55
Coefficient of Thermal Expansion	55
Coefficient of Thermal Conductivity	55
Specific Heat	55
Electrical Properties	56
Electrical Conductivity	56
Dielectric Constant	56
Optical Properties	57
Index of Refraction	57
Chromatic Dispersion	57
Infrared Transmission at 10,000 Å	57
Infrared Limit of Transparency	57

TABLE OF CONTENTS (continued)

	PAGE
Mechanical Properties	58
Ultimate Strength in Compression	58
Ultimate Strength in Tension	58
Outer Fiber Tensile Strength, Transverse Bending	58
Ultimate Strength in Torsional Shear	59
Torsional Creep Rate	59
Young's Modulus of Elasticity	59
Rigidity Modulus, Poisson's Ratio	60
Hardness	60
Microhardness	60
APPENDIX B: ANALYTICAL PROCEDURES FOR DETERMINATION OF Mg ⁺⁺ AND Al ⁺⁺⁺ IN SPINEL	61
APPENDIX C: SLIP CASTING OF SPINEL AND ALUMINA CRUCIBLES	63
APPENDIX D: MATERIAL ANALYSES	65
Chemical Analyses of Raw Materials	65
Basic Magnesium Carbonate, U. S. P. Grade	65
Alumina, Alcoa A-14 Grade	65
Semiquantitative Spectrographic Analyses of Feed Materials for Crystal Growth	66
LIST OF REFERENCES	67

LIST OF FIGURES

FIGURE		PAGE
1	Projections of the idealized spinel lattice on the (111) and (110) planes (after Hornstra, 1960). (a) Projection on (111): the height z' is given in multiples of $1/24 a_o \sqrt{3}$; oxygen ions at $x' = 2$ and $x' = 10$ are omitted. (b) Projection on (110): the length x' is given in multiples of $1/3 a_o \sqrt{2}$. Ions are drawn in thick lines when x' and z' are even numbers and in thin lines when they are odd. The numerals at the left side of (b) correspond with those in the ions of (a) and those at the left of (a) with those in the ions of (b)	7
2	Model of spinel unit cell viewed along [100]	9
3	Model of spinel unit cell viewed along [110]	10
4	Spinel crystal model showing {111} stacking planes	11
5	Spinel crystal model showing intersections of {111} planes	12
6	Temperature dependence of x-ray diffraction intensities for mixtures of irradiated and unirradiated alumina and basic magnesium carbonate calcined for 22 minutes	21
7	Temperature dependence of x-ray diffraction intensities for mixtures of irradiated and unirradiated alumina and basic magnesium carbonate calcined for 60 minutes	22
8	Temperature dependence of x-ray diffraction intensities for mixtures of irradiated and unirradiated alumina and basic magnesium carbonate calcined for 163 minutes	23
9	Isothermal conversion to spinel as a function of $\ln(t)$ for irradiated and unirradiated alumina - basic magnesium carbonate mixtures	24
10	Differential thermal analyses of 700°C precalcined basic magnesium carbonate - alumina batches. Dynamic pure oxygen, atmospheric pressure, 10°C/min. rate	26

LIST OF FIGURES (continued)

FIGURE		PAGE
11	Differential thermal analyses of Batch 2 (Al_2O_3 irradiated) as a function of dynamic gas environment. All materials precalcined at 700°C, 60 minutes	28
12	Pressurized material feeder for crystal growth	39
13	Arrangement for crystal growing with the oxyhydrogen heat source	40
14	Oxyhydrogen crystal growing apparatus with alumina hot-wall furnace	42
15	Cold-wall furnace for oxyhydrogen crystal grower	43
16	Arrangement for crystal growing with the R. F. plasma heat source	45
17	R. F. plasma crystal grower under construction	46
18	Asimuth dependence of microindentation behavior on (001) of Linde synthetic spinel rod, as-polished. Each point is average of 10 Knoop indentations (100g), 0.003" apart along the radius, long axis normal to indicated direction	51

I. INTRODUCTION

The mineral spinel derives its name from the Latin spina (thorn, prickle) because of a characteristic growth habit in naturally occurring deposits in the form of octahedral crystals having hard sharp points. Magnesium aluminate has long been known: to the ancients as a gem mineral, to generations of mineralogists and geologists as a significant mineral, to metallurgists and ceramists as a highly stable mixed oxide refractory, and to a modern generation of ceramists, physicists and electronic engineers as the "model" for the spinel structure, the prototype for magnetically and/or electrically active ceramics of the AB_2O_4 type. In spite of long and intensive study of spinel-structured materials, $MgAl_2O_4$ has been little used as a structural ceramic material. When compared with its two parent oxides, MgO and Al_2O_3 , it is quite apparent that it has been too little used because it is too little understood. Further, it seems apparent that one of the primary reasons has been the lack of single crystals of good quality in contrast to periclase and sapphire. In the figurative sense, spinel has lived up to its thorny, prickly name by resisting efforts to synthesize it in well-characterized stoichiometric single crystal form. Without such crystals, the development of detailed knowledge of its structure and properties commensurate with its potential importance as a useful material in both single crystal and polycrystal forms has long been inhibited.

Single crystals having the spinel structure have been produced commercially for many years by the same Verneuil flame-fusion technique employed in sapphire production and have found use primarily as gem stones and as jewel bearings. But the available crystals, being both non-stoichiometric (alumina-rich) and impure (generally containing colorant oxides), have not been considered suitable for research purposes so that relatively little reliable property data have become available, particularly in the area of mechanical behavior. Dislocation configurations and orientations, while predicted on theoretical grounds, and deduced in part from indentation hardness experiments and the like, still lack experimental confirmation and, indeed, suitable etch pit techniques are only now being developed to aid in the characterization of dislocation distributions.

This report reviews the accomplishments- and the remaining problems- of the first eighteen months of work on a research program concerned with the closely related (and interrelated) processes of crystal growth and crystal deformation in spinel.

The objectives of the research herein reported have been:

To conduct theoretical and experimental investigations of growth and deformation processes in magnesium aluminate spinel in pure and alloyed single crystal forms.

Manuscript released for publication as an ASD Technical Documentary Report
January 1963.

To evolve methods for growing single crystals of magnesium aluminate spinel of high purity in essentially stoichiometric proportions, as well as those having controlled levels of alloying cations and/or non-stoichiometry, and to determine the parameters governing the methods employed.

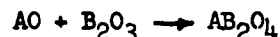
To determine the relationships existing during mechanical deformation between the purity and structural states (i.e., of the "perfect" lattice and of the crystalline defects) of such crystals and (a) the states of stress and strain, (b) the rates and duration (and/or cyclic character) of loading (c) the temperature, (d) atmospheric environment, and (e) surface conditioning. Both macro- and micro-scale testing will be employed, as best suits the nature of the problem.

To seek a better understanding and if possible, experimental confirmations of mechanisms capable of permitting (or of precluding) room temperature plastic deformation in single crystal spinel when subjected to externally applied stresses which are insufficient to induce failure by fracture.

Work has proceeded along several different avenues, ranging from very practical matters of developing and bringing together suitable materials, apparatus, and process technology in the prosecution of an actual research program in crystal growth, through fundamental considerations of the role of defects of various classes in the reaction kinetics of spinel formation, in crystal growth, and in deformation processes. The main sections of this report contain pertinent technical findings, interpretations of results whenever justifiable, and selections of most fruitful directions for a continuing program of research. The Appendix contains a selection of useful and detailed information relating to spinel, including its properties, preparation, and analysis, as well as supporting information on procedures and equipment employed in the research program.

II. SPINEL FORMING REACTIONS

According to Anderson (1952) materials with the spinel structure were synthesized as early as 1850. Experimentally, many workers have shown that spinel is initially formed according to the equation



at temperatures above $\approx 900^\circ\text{C}$ on the surface of contact between the respective oxides. Wagner (1936) suggested that further growth occurs by diffusion of cations A^{++} and B^{+++} in opposite directions through the spinel layer and that the oxygen ions are practically immobile. Wagner's concept was predicated on two observations: (1) X-ray studies showed the oxygen ions in spinel form a well-ordered face-centered cubic lattice whereas the cations are distributed somewhat irregularly through the lattice (Barth and Posnjak, 1932 and Machatschi, 1932) and (2) the reacting cations have considerably smaller ionic radii than the oxygen ions, e.g., Evans (1952) reports Goldschmidt's ionic radii values $r_{Mg^{++}} = 0.78\text{\AA}$, $r_{Al^{+++}} = 0.57\text{\AA}$ and $r_{O^{--}} = 1.32\text{\AA}$.

Fisher and Hoffman (1954) reported an experiment wherein cylinders of $FeAl_2O_4$ and Al_2O_3 were placed into contact for 50 to 100 hours at 1500°C . They observed a contraction of the Al_2O_3 cylinder in the diffusion zone which they believe gives evidence that the Al^{+++} cations diffuse faster than the Fe^{++} cations. Linder et al. (1955, 1956) by means of marker studies concluded that $ZnFe_2O_4$, $ZnCr_2O_4$, $NiCr_2O_4$ and Zn_2SnO_4 form by the Wagner mechanism and that $ZnAl_2O_4$ and $NiAl_2O_4$ were formed by diffusion of the A^{++} cations and O^{--} ions through the aluminate. In contrast, Carter (1961) showed by means of inert markers that the formation of $MgAl_2O_4$ from Al_2O_3 and MgO in a hydrogen atmosphere at 1900°C followed the Wagner mechanism, i.e., counter diffusion of Al^{+++} and Mg^{++} through the reaction area.

Fuerstenau, Fulrath and Pask (1961, 1962) reacted single crystals of MgO and Al_2O_3 in air at 1560°C for 250 hours by placing polished faces together. The spinel formed at the interface consisted of three distinct sublayers: a thin sublayer of spinel next to the MgO formed from the original MgO crystal, a center sublayer which formed from the sapphire, and a lower sublayer of sapphire showing strain. The thickness of the spinel formed from the MgO was only about one-tenth of the thickness of that formed from the sapphire, indicating that the magnesium ions may diffuse much more rapidly in Al_2O_3 than aluminum ions diffuse through MgO . They also reported an epitaxial growth relationship between the sapphire and the spinel grown from the sapphire, with the (111) $[110]$ of spinel and the (0001) $[1010]$ of $\alpha\text{-}Al_2O_3$ being congruent. In an oxidizing atmosphere, Al_2O_3

and MgO react to form spinel at the area of contact between the two, thus permitting only bulk diffusion to occur. Carter has shown this is also true of MgO and Fe_2O_3 in an oxidizing atmosphere.

Navias (1961) and Carter have both demonstrated that in the temperature range of 1500 - 1900°C in a hydrogen atmosphere the formation of spinel is by a solid-gas reaction, that probably MgO is transferred as the gaseous element, and that the rate of reaction is a function of temperature. In later experiments Navias (1962) showed that a reduction in hydrogen pressure (at 1800°C) caused only a minor reduction in the rate of spinel formation. A substitution of argon for hydrogen greatly reduced the spinel formation and resulted in an erratic distribution of reaction sites. In vacuum (0.1 to 4×10^{-4} mm Hg) thin but uniform coatings of spinel were formed on sapphire exposed to the evacuated furnace surroundings, while on samples totally enclosed in periclase containers the coatings were substantially thicker and in two instances approached equal thicknesses to those obtained in hydrogen atmosphere.

Fuerstenau et al. in their spinel formation studies between single crystals of sapphire and MgO in an air atmosphere found that both mechanisms of transport of MgO across the spinel interface occurred when there was misfit between the two original crystals, i.e., where the two were in contact spinel was formed by the diffusion mechanism and where contact was not made, spinel grew from the vapor and after contact was made the spinel formation continued by the diffusion mechanism. Under the conditions of these experiments the vapor mechanism has the slower growth rate.

From the foregoing discussion five significant facts are quite apparent: (1) MgAl_2O_4 spinel can be readily formed at elevated temperatures from its constituent oxides, MgO and Al_2O_3 , (2) the specific mechanism of spinel formation takes place by counterdiffusion of the cationic species through the spinel reaction zone, (3) the relative rates of diffusion have not been unambiguously determined and therefore the rate determining cation has not been clearly established, (4) the atmospheric environment has a profound effect upon the overall rate of spinel formation, and (5) in non-oxidizing environments, the overall reaction is modified and accelerated by (a) vapor transport processes which in effect increase the concentration of the reacting constituents and (b) enhanced mobilities within the solid phases due to excess vacancies.

Active interest in these matters during the present research has been concentrated in three areas. Since it has been necessary to produce in some quantity spinel feed materials of controlled stoichiometry, small particle size, and a reasonably high degree of purity, first emphasis has been placed on the utilization and control of spinel-forming reactions. This work is the subject of Section IV, "SYNTHESIS OF SPINEL FEED MATERIALS." The inherent role of

defects in spinel forming reactions as well as in growth and deformation processes in crystalline spinel has stimulated an investigation of the role of fugitive defects, e.g., vacancies, in such processes. These results are described and discussed in Section V, "EFFECT OF RAW MATERIAL IRRADIATION ON SPINEL FORMATION." Finally, there has been a continuing, overall interest in the kinetics and thermodynamics relating to spinel, its raw materials, and its analogous compounds.

III. STRUCTURE AND PROPERTIES OF MAGNESIUM ALUMINATE SPINEL

Structure of Spinel

Ideal Structure. The ideal structure of spinel is one of a face centered cubic close packing of oxygen ions with metal ions in the interstices. The unit cell of spinel consists of 32 oxygen ions with 32 octahedral (B) sites, 16 of which are filled with aluminum ions and 64 tetrahedral (A) sites, eight of which are filled with magnesium ions. This idealized structure of spinel is shown projected on the (111) plane in Figure 1(a) and on the (110) plane in Figure 1(b). Using Hornstra's (1960) notation the height, Z' , of the ions above the plane is expressed in multiples of $1/24 a_o \sqrt{3}$ (a_o = lattice constant) in order to obtain whole numbers. In Figure 1(a) Hornstra chose the zero point of height as lying in a layer of cations at the octahedral (B) sites, so that these ions and the oxygen ions would be at even heights with the tetrahedral ions (A-sites) lying at odd heights.

At $Z' = 4$ only three-fourths of all the octahedral positions are filled with none of the tetrahedral sites at $Z' = 3$ and 5 being occupied. The layer structure of the cations at $Z' = 4$ has been denoted as a kagome layer by Iida (1957). Figure 1(a) shows the arrangement of these ions into hexagons and triangles. Between the oxygen layers at $Z' = 6$ and $Z' = 10$, cations of both kinds are found. Although these cations are at three different heights and do not actually form a layer, this composite layer is called a mixed cation layer. Between the close packed oxygen layers in a $\langle 111 \rangle$ direction alternate kagome layers and mixed layers are found.

The tetrahedral ions at $Z' = 7$ and $Z' = 1$ which are nearest to a kagome layer ($Z' = 4$) occupy sites above and below the empty sites which lie in the centers of the hexagons of the kagome layer. In Figure 1(a) the projections of the cations at $Z' = 8$ and $Z' = 9$ coincide with the centers of the triangles of the kagome layer at $Z' = 4$.

A projection of the idealized spinel structure on the (110) plane is shown in Figure 1(b). In this projection the layer at $X' = 4$ is a repeat of the layer of $X' = 0$.

In Figure 1(a) and (b) it can be seen that every oxygen ion in the spinel lattice is surrounded by three aluminum ions at octahedral sites and one magnesium ion in a tetrahedral site. This arrangement satisfies the conditions of Pauling's rule -- that the valency of an anion is equal to the sum of the valencies of the cations surrounding it divided by their respective coordination numbers.

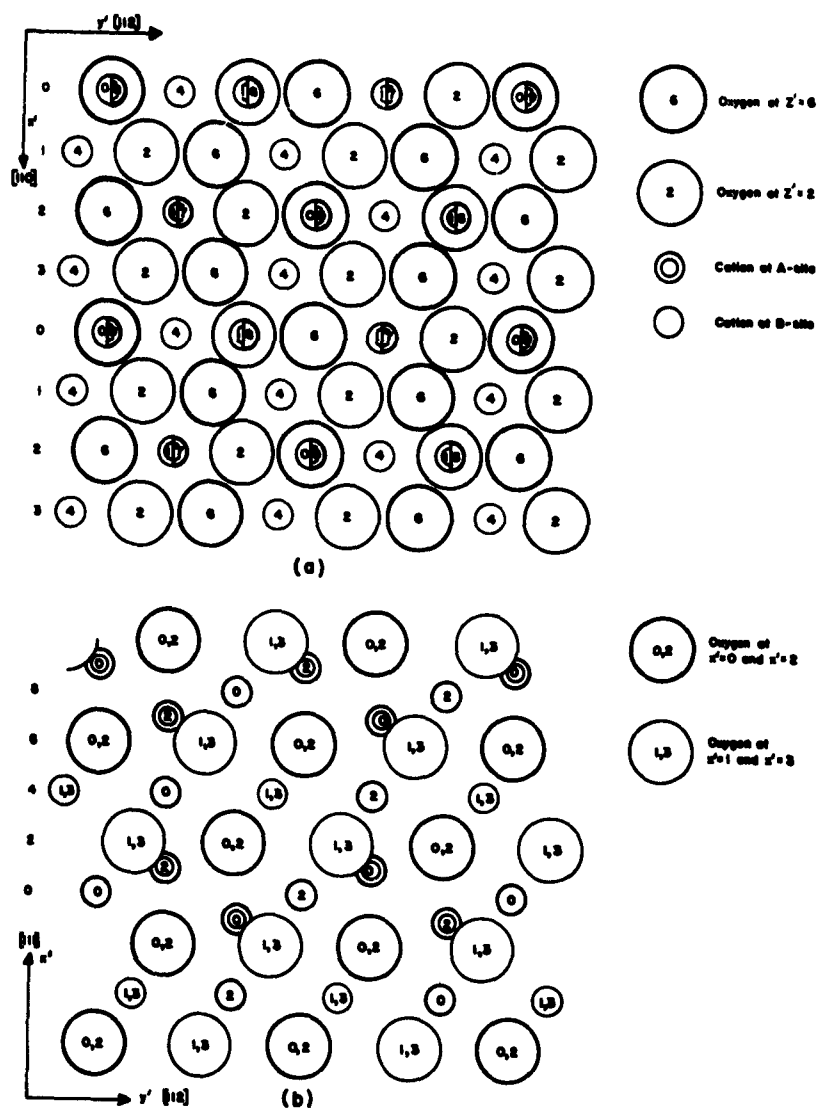


Figure 1. Projections of the idealized spinel lattice on the (111) and (110) planes (after Hornstra, 1960). (a) Projection on (111): the height z' is given in multiples of $1/24 a_0 \sqrt{3}$; oxygen ions at $x' = 2$ and $x' = 10$ are omitted. (b) Projection on (110): the length x' is given in multiples of $1/3 a_0 \sqrt{2}$. Ions are drawn in thick lines when x' and z' are even numbers and in thin lines when they are odd. The numerals at the left side of (b) correspond with those in the ions of (a) and those at the left of (a) with those in the ions of (b).

To assist in studies involving crystal structure and crystal orientations, three-dimensional atomic models have been prepared using wooden balls of appropriate sizes on vertical wires held in plastic bases.¹

Figures 2 and 3 illustrate a model of the unit cell of stoichiometric spinel containing eight molecules, i.e., $\text{Mg}_8\text{Al}_{16}\text{O}_{32}$, constructed with an expanded (2x) lattice for improved visibility.

The cubic symmetry (cube axes parallel to model axes) is quite apparent in Figure 2 where the view is along [100]. In Figure 3, the view is along [110]. The largest balls represent oxygen ions, the smallest represent the aluminum ions, and the medium sized ones represent the magnesium ions. Although the unit cell model contains all elements of the structure, neither the repeat symmetries of cation configurations nor the (111) planes of special interest in both growth and deformation processes can be visualized easily from such a simple model. Therefore a larger model whose orthogonal axes are the [111], $[\bar{1}\bar{1}0]$ and $[\bar{1}\bar{1}2]$ has been constructed, and is illustrated in Figures 4 and 5. Additional details on the formal structure designation of spinel may be found in the Appendix A.

Actual Structure. The actual arrangement of the ions in magnesium aluminate deviates slightly from that of the idealized structure. Bacon (1952) used a neutron-diffraction technique to demonstrate that the cation arrangement of polycrystalline spinel corresponded closely with the idealized structure, but the oxygen parameter, u , was 0.337 rather than the 0.375 of the idealized close-packed oxygen lattice. This increase in the oxygen parameter corresponded to a net movement of the oxygen ions from their nearest tetrahedral interstice. A consideration of the ionic radii of the ions demonstrated the necessity of the interstice being enlarged for the magnesium ion to "fit."

By Fourier analysis Jagodzinski and Saalfeld (1958) found that the structure of a natural spinel was approximately the same as that reported by Bacon, but there were a considerable number of faults present. Stoichiometric synthetic spinel single crystals only approximated the normal spinel structure with a large number of faults being present.

Brun, et al. (1960), using measurements of the paramagnetic nuclear resonance of ^{27}Al , determined that the octahedral sites of natural spinels were almost exclusively occupied by aluminum ions. However, the results from synthetic stoichiometric spinels indicated that the magnesium and aluminum ions were in a highly disordered distribution on the tetrahedral and octahedral sites.

¹This system of model construction was adapted from one devised by Dr. Pol Duwez, California Institute of Technology, Pasadena, California. In these particular models, 1A = 0.568 in., i.e., oxygen, with an ionic diameter of 2.64A, is represented by a wooden sphere 1.5 in. in diameter.

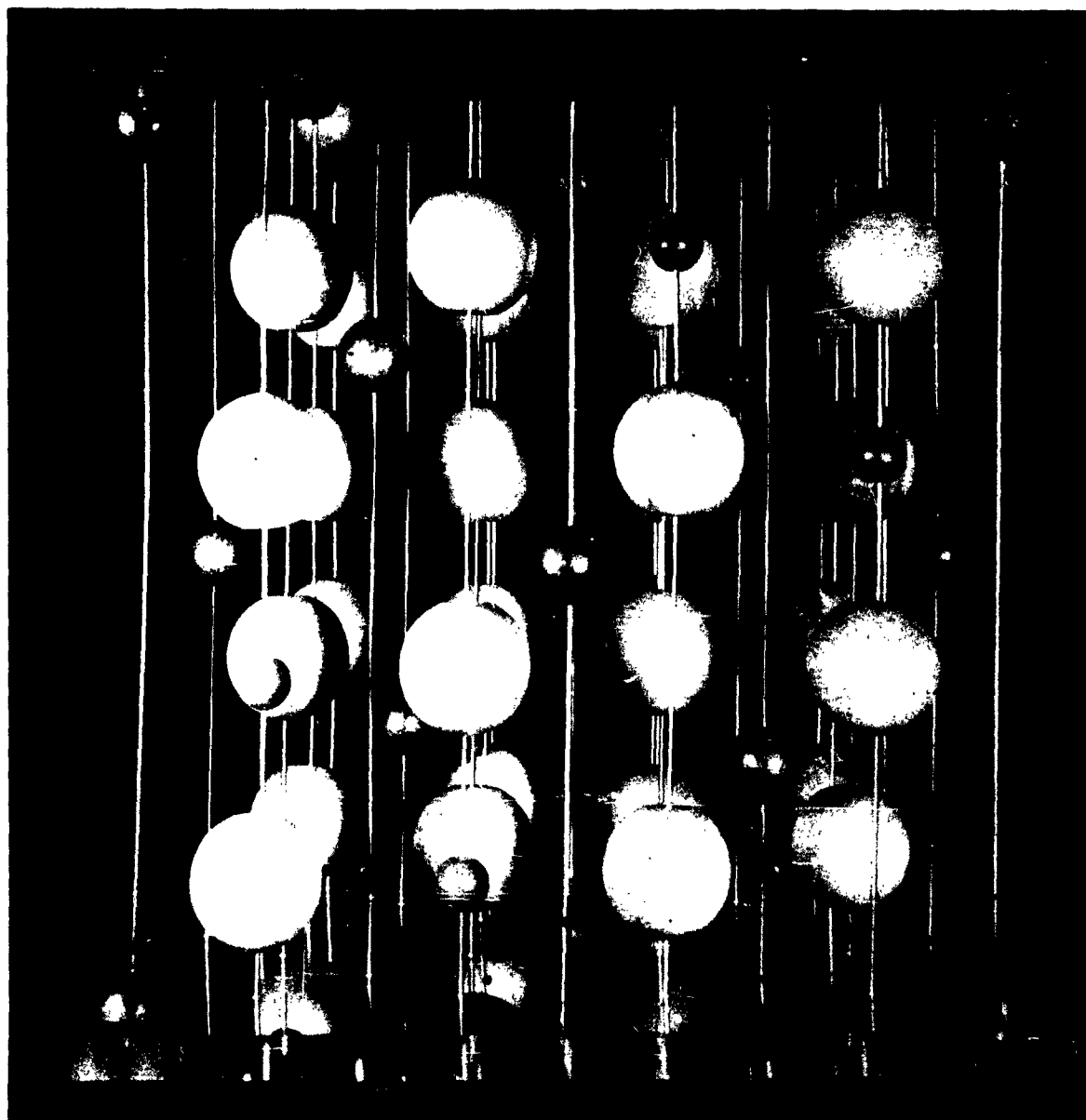


Figure 2. Model of spinel unit cell viewed along $[100]$.

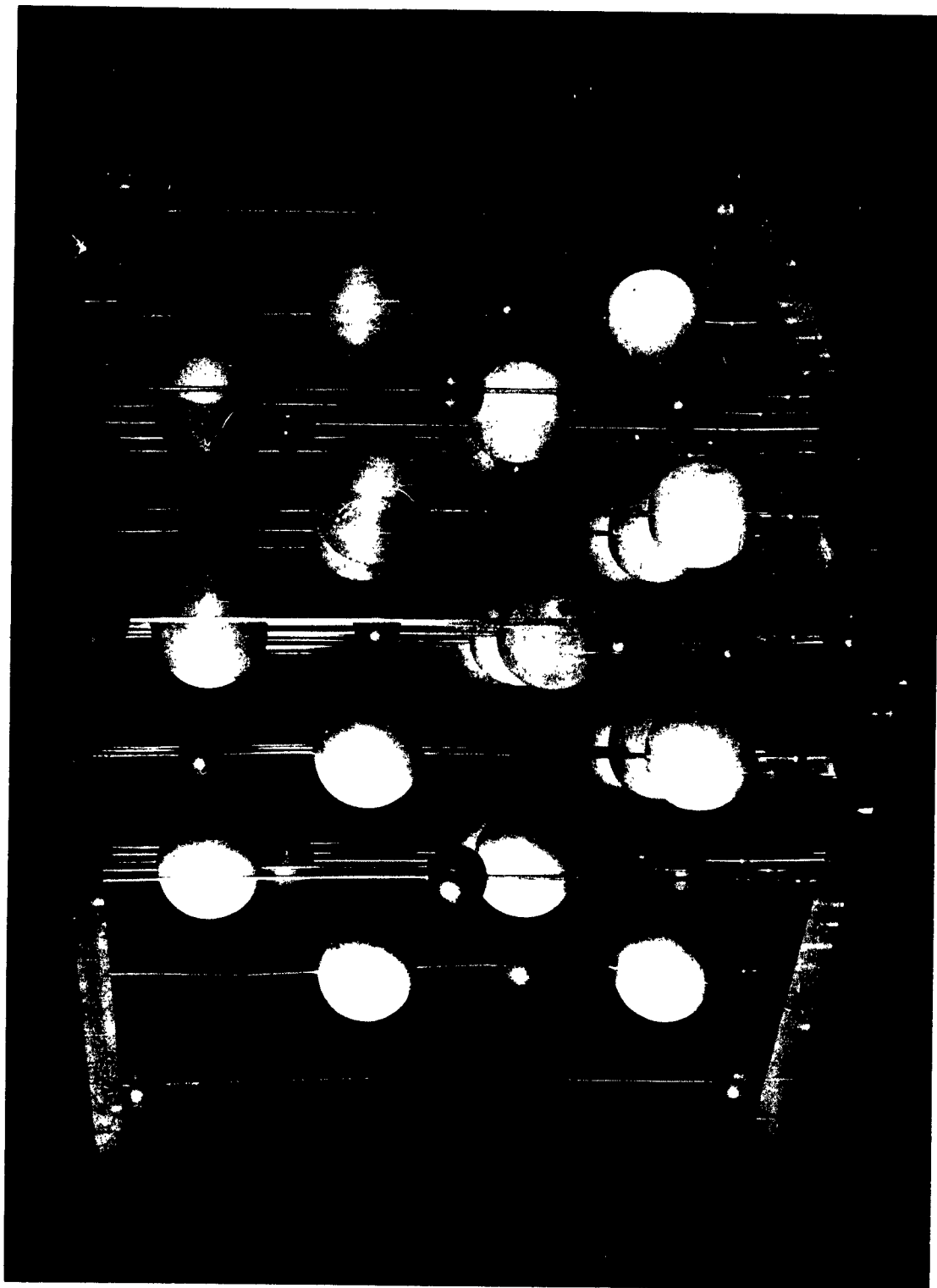


Figure 3. Model of spinel unit cell viewed along $[110]$.



Figure 4. Spinel Crystal model showing $\{111\}$ stacking planes.



Figure 5. Spinel crystal model showing intersections of $\{111\}$ planes.

Furthermore, if a natural spinel crystal was heated at 800-900°C, it became disordered and could not be reordered.

Dislocations in the Ideal Structure. Hornstra (1960) predicted a dislocation model for spinel which later was verified by transmission electron microscopy (Hornstra 1962). This model involves the passage of $\langle 112 \rangle$ quarter-partial dislocations along the $\{111\}$ slip planes with total Burgers vectors being in $\langle 110 \rangle$ directions. Since the oxygen ions fit so well in the intermediate positions during the passage of a dislocation in the slip plane there are certain regions where they occupy these wrong positions. These regions of stacking faults are bounded by either two partial dislocations or a partial dislocation and the perfect lattice. Therefore, a total dislocation in a $\{111\}$ slip plane may consist of four $\langle 112 \rangle$ partial dislocations and three stacking faults with a total Burgers vector of $[110]$.

Twinning. The spinel structure is well known for its $\{111\}$ twins, the so-called spinel twins. Macroscopically, twinning may be described as reflection with respect to a $\{111\}$ plane or as a rotation around $[111]$ by 60° or 180°, or even as a rotation of 180° about a $\langle 112 \rangle$ axis (Hornstra, 1960). Microscopically the mirror plane may be a glide plane and the twin axis need not coincide with a three fold axis. A close relation exists between stacking faults and twins, as stacking faults may often be considered as extremely thin twin lamellae.

Alumina-rich Spinel. As previously pointed out, Jagodzinski and Saalfeld (1958) determined that synthetic spinels showed deviations from the normal structure. They also found that the greater the amount of alumina present, the greater the deviation. Their technique showed that the excess vacancies, created by the introduction of alumina, occurred at the sites of the aluminum ions. Jagodzinski and Saalfeld also determined that the nonstoichiometric spinel crystals, as well as the stoichiometric spinels, did not strictly obey the symmetry rules of the space group $Fd \bar{3}m$ (O_h^7). The interpretation given was that the spinel crystals were actually composed of twinned crystallites of lower symmetry.

Solid Solutions in the $MgO-Al_2O_3$ System

In the original phase equilibria studies of the system $MgO-Al_2O_3$, Rankin and Merwin (1916) reported that $MgAl_2O_4$ formed a nearly complete series of solid solutions with $\alpha-Al_2O_3$. Roy, et al. (1953) essentially reconfirmed the earlier finding but by hydrothermal means delineated the low temperature (down to 700°C) limits of solubility. They also reported the maximum solid solution as 86 mol % Al_2O_3 (≈ 94 wt. %) which was in reasonable agreement with Clark, et al. (1934).

Rankin and Merwin showed no solid solution existing between MgO and $MgAl_2O_4$. Recently Alper, et al. (1962) reported periclase solid solution with a maximum of 18% Al_2O_3 (9.5% Al^{+++}) and a maximum solid solution of 11% MgO (6% Mg^{++}) in $MgAl_2O_4$. They showed a slight, although important modification of the liquidus.

Rankin and Merwin also reported that " β - Al_2O_3 " did not form solid solutions with MgAl_2O_4 but a limited solubility of MgAl_2O_4 was formed in the " β - Al_2O_3 ." "...under identical conditions of melting and cooling sometimes the solid solution will be formed, sometimes, the $\text{MgO} \cdot \text{Al}_2\text{O}_3$ along with β - Al_2O_3 ." Beevers and Ross (1937) found the so-called " β -alumina" to be not a form of alumina but a compound having a molal ratio of $\text{Al}_2\text{O}_3:\text{Na}_2\text{O}$ (or K_2O) of 11:1. Thus it could well be that Rankin and Merwin were working with contaminated materials.

In an earlier section mention was made that Fuerstenau, et al. (1961) in their solid state reactions of MgO and Al_2O_3 found a sublayer of sapphire showing strain which was attributed to a probable supersaturation of magnesium ions in the sapphire. In high temperature doping of sapphire with NiO , Palmour and Krieger (1961) showed (with the assistance of a microprobe analysis carried out at California Institute of Technology²) a measurable diffusion of NiO into the sapphire past the spinel-sapphire interface. The plot followed a normal diffusion gradient within this region, and correlations were established between this gradient and the microindentation behavior. It would seem reasonable that a similar "alloying" of sapphire would occur with MgO , particularly in view of the fact that the ionic radii are reported to be the same, i.e., 0.78A.

Exsolution in Nonstoichiometric Spinel

Mechanism of Exsolution. Rinne (1928) noticed upon heat treatment at 800°C for five hours that the alumina-rich ($\text{Al}_2\text{O}_3:\text{MgO} = 3.5:1$) spinel crystals showed a clouding effect. Through further experimentation Rinne learned that no appreciable optical effect could be detected with tempering up to 1050°C for thirty minutes, but with longer times the crystal became slightly opaque. This opacity increased and after fourteen hours of heating, what Rinne interpreted as **colloidal** particles appeared. By optical techniques Rinne determined that the $\{311\}$ plane was the precipitation plane for the **colloidal** particles. Upon further heat treatment it was noted that the **colloidal** particles converted to α -alumina with the (0001) plane of α -alumina and the (111) plane of spinel coinciding. The formation of α -alumina led Rinne to believe that the **colloidal** particles which first appeared were γ -alumina.

Saalfeld and Jagodzinski (1957) confirmed Rinne's observation of the two precipitating planes and of the final precipitate (α - Al_2O_3), but their findings disagreed with Rinne's as to the intermediate precipitate. In Saalfeld and Jagodzinski's detailed study of the exsolution of alumina from spinel they listed

²Personal communication, Dr. Pol Duwez, 1960.

the three states of exsolution as:

1. The state of pre-exsolution.
2. The formation of a monoclinic intermediate structure.
3. Final exsolution of α -alumina.

The state of pre-exsolution, after rapid cooling from growth temperature, exists in all synthetic crystals with molar ratios of Al_2O_3 to MgO of 1:1 to 4:1 and was detected by the diffuse diffraction pattern of the spinel crystal. These diffuse diffraction patterns were caused by short-range ordering effects which represent noticeable deviations from the normal spinel structure. One important observation was the presence of the same type of lattice defects in stoichiometric spinel ($\text{MgO} \cdot \text{Al}_2\text{O}_3$) as was noted in the alumina-rich spinels. Whether this was due to local inhomogeneities in the crystal or whether it was due to temperature scattering was not established.

In spinel crystals with molar ratios of Al_2O_3 to MgO of 1.7:1 the pre-exsolution state remains regardless of the temperature or time at temperature. With a molar ratio above 1.7:1 but below 2.5:1 no intermediate phase was detected, but exsolution of α - Al_2O_3 still took place.

The intermediate structure first began to form around 800°C in the 2.5:1 to 4:1 spinels. Between 800 to 900°C several interpenetrating lamellae began to appear. In 5:1 to 7:1 spinels these lamellae existed even in untempered spinel boules. After being heated to around 1000°C the intermediate structure was completely developed.

The exsolution of α -alumina took place in crystals heated above 1000°C for long times and above 1200°C for very short times. Exsolution on the surface took place at defect sites, yielding crystallites which were not specifically oriented, while within the crystal, α -alumina platelets formed along the traces of the lamellae of the intermediate structure, with their basal planes coinciding with the $\{111\}$ spinel planes. When the spinel- α -alumina mixture was heated above 1300°C, the alumina began to go back into solution.

Jagodzinski (1957) determined by a Fourier analysis that the structure was a monoclinically distorted cubic packing of the oxygen ions with a large number of octahedral interstices occupied. The molecular formula was given as $\text{Mg Al}_{26}\text{O}_{40}$ which corresponds to an $\text{MgO}:\text{Al}_2\text{O}_3$ molecular ratio of 1:13. However, Jagodzinski was quick to point out the many difficulties involved in, and assumptions necessary for, the structural analysis.

Effect of Exsolution on Mechanical Properties. Eppler (1943) investigated the effect of tempering on the erosion (sand-blasting) hardness of $\text{MgO} \cdot 3.5 \text{Al}_2\text{O}_3$ spinel and found that the hardening increased to a maximum after twelve hours at $1,000^\circ\text{C}$ and then decreased back to the normal value. This maximum hardness was reached faster as the temperature was increased. Eppler's measurements were made on large crystals and no consideration was given to the possible anisotropy of spinel.

Mangin and Forestier (1956) studied the effect of the variation of time and temperature on the hardening of single crystal spinel ($\text{MgO} \cdot 3.65 \text{Al}_2\text{O}_3$). The effect was detected (on a constant, but unspecified orientation) by Knoop micro-hardness with a load of 1,000 grams. Mangin and Forestier observed an increase in hardness from about 1120 at room temperature to a maximum of 1320 Knoop hardness decreasing with increasing temperature. It was noted that the hardening was accompanied by an oriented precipitate which was not α -alumina. Alumina was detected above 1050°C and did not appear to be associated with the hardening phenomena.

Properties of Spinel

The physical and chemical properties of magnesium aluminate spinel are best known from the polycrystalline material and have been recently reviewed by Ryshkewitch (1960). Rigby (1953) has discussed the structural chemistry and physical properties of the broad family of spinel-structured materials. An unpublished thesis by Anderson (1952) specifically treats the preparation and properties of sintered magnesium aluminate spinel. Palmour, *et al.* (1962 a, b), working with hot pressed MgAl_2O_4 , have reported room temperature transverse strength of about 34,000 psi in four point loading for fine grained dense material, almost twice as high as Ryshkewitch's value and almost three times higher than Anderson's. All three reports agree on a Young's modulus value of about 34×10^5 psi at room temperature.

As previously mentioned, there are only limited data in the literature on physical properties of spinel single crystals. The detailed paper by Rinne (1928) is still one of the major sources of information on the growth and properties of non-stoichiometric spinel crystals. More recently, Wickersheim and Lefever (1960) have described optical absorption spectra of spinel single crystals. Appendix A includes a summary of property data of interest in this study, as obtained by various investigators from both polycrystalline and single crystal materials.

IV. SYNTHESIS OF SPINEL FEED MATERIALS

The stoichiometry and purity of spinel feed materials are major factors in determining the quality of single crystals being grown from them. The physical character of the feed material also is important in establishing control of the growth operation. Consequently, detailed studies are underway of spinel-forming reactions capable of producing uniform feed materials of high purity, predetermined stoichiometric ratios, and controlled particle (and/or agglomerate) size.

Mechanically Mixed Oxides

A batch of Linde's sapphire boule powder and Phillip Carey basic magnesium carbonate calculated to yield a 1:1 mole ratio of $MgO:Al_2O_3$ was prepared. This batch of extremely light and fluffy material was then dry-blended in a twin-shell blender. After blending, the mixture was placed in a large covered alumina crucible and fired to $1150^{\circ}C$ for 2 hours. After calcination, the product was X-rayed and found to contain nothing but spinel. The product was fairly friable, but did contain some rather tough agglomerates. It was necessary to screen these agglomerates out before the material could be used as feed material.

This material appeared to feed adequately, but successful growth has not been obtained with it. Whether this is due entirely to the higher melting point of the stoichiometric material or partially due to the nature of the feed material has not been clearly determined.

Stoichiometric feed material was also prepared by ball milling Phillip Carey basic magnesium carbonate and Alcoa A-14 alumina in 1:1 mole ratio in distilled water in a high-alumina mill using alumina balls. After milling, the material was dried and then calcined at $1450^{\circ}C$ for 1 1/2 hours. After calcination the material was remilled for 1 1/2 hours. This material did not prove to be a satisfactory feed material as it "packed" in the track of the Syntron bowl under the influence of vibratory motion.

Coprecipitated Hydroxides

As a preliminary step to the preparation of stoichiometric spinel feed materials, several intermediate coprecipitates were prepared in small quantities ($\approx 100g$) by using different magnesia to alumina mole ratios ranging from 1:1.1 to 1:3.5. For this purpose, solutions of reagent grade hexahydrated aluminum chloride

and hexahydrated magnesium chloride in the desired ratios were prepared in 95% ethyl alcohol (Stocker and Collonques, 1957). Upon addition of ammoniacal 95% ethyl alcohol to such solutions, aluminum hydroxide and magnesium hydroxide were co-precipitated. The reaction was carried out in a polypropylene container to minimize silica contamination, and with vigorous agitation to insure uniformity of product. After filtering and drying, the combined hydroxides of aluminum and magnesium were calcined for 24 hours at temperatures over the 700°-1140°C range in covered high alumina or spinel crucibles, yielding friable white powders. X-ray analyses and preliminary studies of performance during crystal growth suggest that 790°C is near-optimum calcining temperature.

Pilot Production

On the basis of these experiments, the coprecipitation technique now is being scaled up for production of pilot quantities of spinel feed materials, i.e., lots yielding 500 to 1000 grams of calcined spinel. Precipitation from alcohol, while quite reliable and controllable, does present some hazards and difficulties since during the drying of a large batch several gallons of alcohol must slowly be removed from the gelatinous coprecipitate. An alternative procedure involving coprecipitation from aqueous solution in conjunction with spray drying prior to calcination has been successfully carried out, and is being developed for pilot production.

Investigations of the synthesis of spinel feed materials have been closely associated with two supporting research activities, each making a significant contribution toward the goals expressed here, and each technically complex enough to warrant detailed discussion of the problems involved as well as the progress made in solving them. These activities are described in APPENDIX B, Analytical Procedures for Determination of Mg^{++} and Al^{+++} in Spinel, and APPENDIX C, Slip Casting Large Alumina and Spinel Crucibles.

V. EFFECT OF RAW MATERIAL IRRADIATION ON SPINEL FORMATION

Theoretical Considerations

The formation of spinel from MgO and Al_2O_3 has long been recognized as a solid state process. Only recently has it been established that the essential mechanism is that of counter diffusion of the two cation species through an essentially close-packed oxygen lattice. The possible role of irradiation-induced vacancies and other defects in altering the rates of reaction in spinel formation was suggested by earlier experiments of Choi, McBrayer and Palmour (1961) in which irradiation induced defects modified the micromechanical deformation behavior of sapphire, apparently by means of altered mobilities of slip and twinning dislocations.

In considering low-level irradiation damage in sapphire or in spinel the cation vacancies and/or interstitials produced bring about only an incremental increase (or rearrangement) in the already large population of cation vacancies present in the structure. In contrast, it may be reasoned that any anion vacancies produced by irradiation would effect a substantial change in the population of such defects in the close-packed oxygen framework. If anion and cation vacancies are produced in reasonably equivalent numbers by irradiation then the energy storage due to irradiation damage within such materials seems most likely to be concentrated in the excess anion defects rather than in some additional scrambling of the cations.³ Thus irradiation may be considered as a means of achieving a virtual oxygen deficient state at room temperature, and without side reactions as is frequently the case with chemical reduction at elevated temperatures. Because of the importance attached to the state of oxidation (see Section II, Spinel Forming Reactions) and the problems associated with stoichiometry in spinel, experiments with such irradiated materials are considered particularly pertinent not only to the matter of developing controlled methods of producing spinel feed materials but to a better understanding of the mechanisms involved in the spinel forming process. When it is considered that alumina and magnesia sustain detectable damage at relatively low dosages ($\approx 10^{15}$ nvt), that the radioactive species have very short half-lives, permitting safe handling after a reasonable "cool-off" period, and that the irreversible formation of spinel is easily followed by various experimental techniques, spinel appears to provide a uniquely favorable system for investigating the mechanisms of interest.

³The essential chemical similarity between anion vacancies and stable cation interstitials permits both cases to be treated in this discussion as oxygen vacancies. It is recognized that the physical configurations and energy states are not totally equivalent.

Experimental Procedure

Alcoa A-14 alumina⁴ and basic magnesium carbonate⁴ (B.M.C.) were separately irradiated in a heterogeneous reactor for 10 hours at 10KW ($\approx 5.4 \times 10^{15}$ fast neutrons/cm²) and were allowed to "cool off" to a level of negligible radioactivity (attributable only to trace impurities of radioactive Na and Fe). From the irradiated and comparable unirradiated materials four batches were mixed in 1:1 stoichiometric ratio and milled in acetone for 12 hours in an alumina ball mill.

<u>Batch No.</u>	<u>Alumina</u>	<u>Basic Magnesium Carbonate</u>
1	irradiated	irradiated
2	irradiated	unirradiated
3	unirradiated	irradiated
4	unirradiated	unirradiated

After evaporation of the acetone, the dry material was accurately weighed (\approx 1-gram samples) into covered, high-purity alumina crucibles, and each of the four batches was calcined according to a statistical design involving nine firing temperatures over a range from 700-1500°C and three soak times over a range from 22-163 minutes, (a total of 27 test points for each batch). All firings were made in a Kanthal-Super kiln (MoSi₂ elements). The specimens were heated at an essentially constant rate to the soak temperature, and were withdrawn and air-quenched at the end of the soak period.

The calcined samples were x-rayed with a Norelco diffractometer on slow scan (1°/min.) with a scintillation counter adjusted for minimum background, using MoK_α radiation (50 Kv, 18 ma). A weighing technique was employed to determine the integrated intensities of the (220) spinel and (1014) Al₂O₃ lines; d-values were also determined but remained essentially constant for each of the peaks in question. The integrated intensities were also checked against the corresponding maximum peak heights for each run and were found to be consistent in all cases.

Experimental Findings

X-ray Evidence of Spinel Formation. Figures 6, 7, 8, and 9 illustrate changes in integrated intensities as functions of firing time and temperature

⁴See Appendix D for analyses.

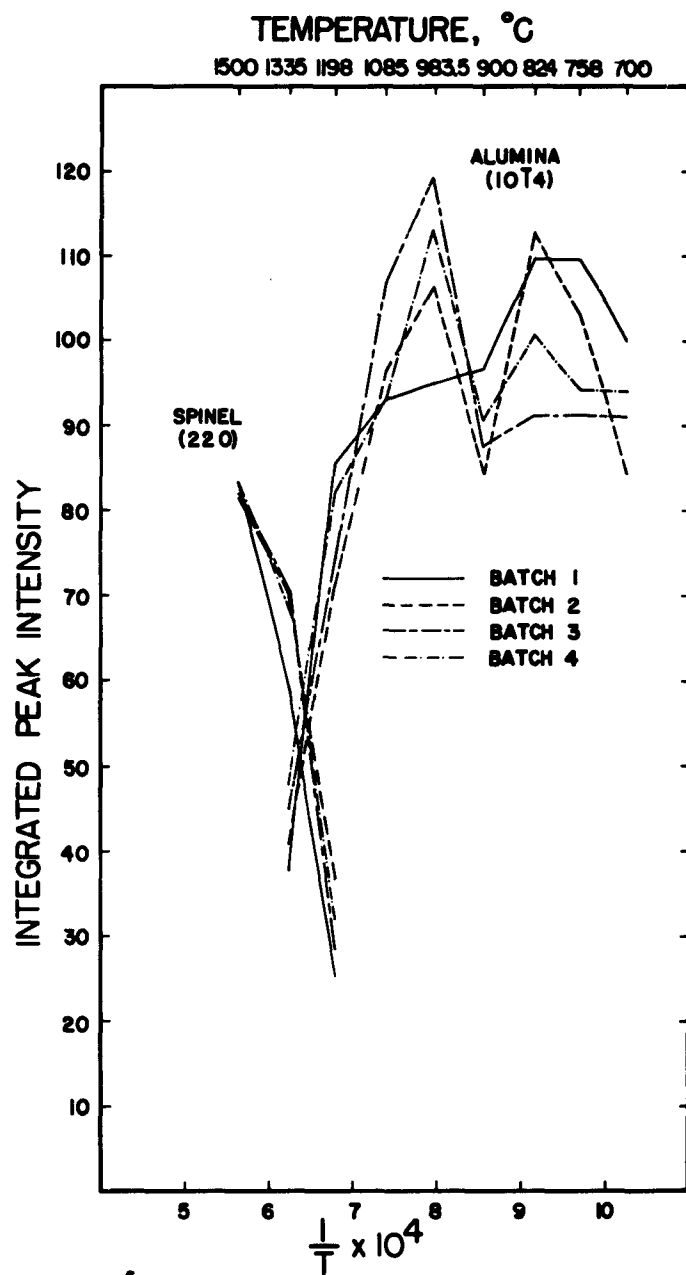


Figure 6. Temperature dependence of x-ray diffraction intensities for mixtures of irradiated and unirradiated alumina and basic magnesium carbonate calcined for 22 minutes.

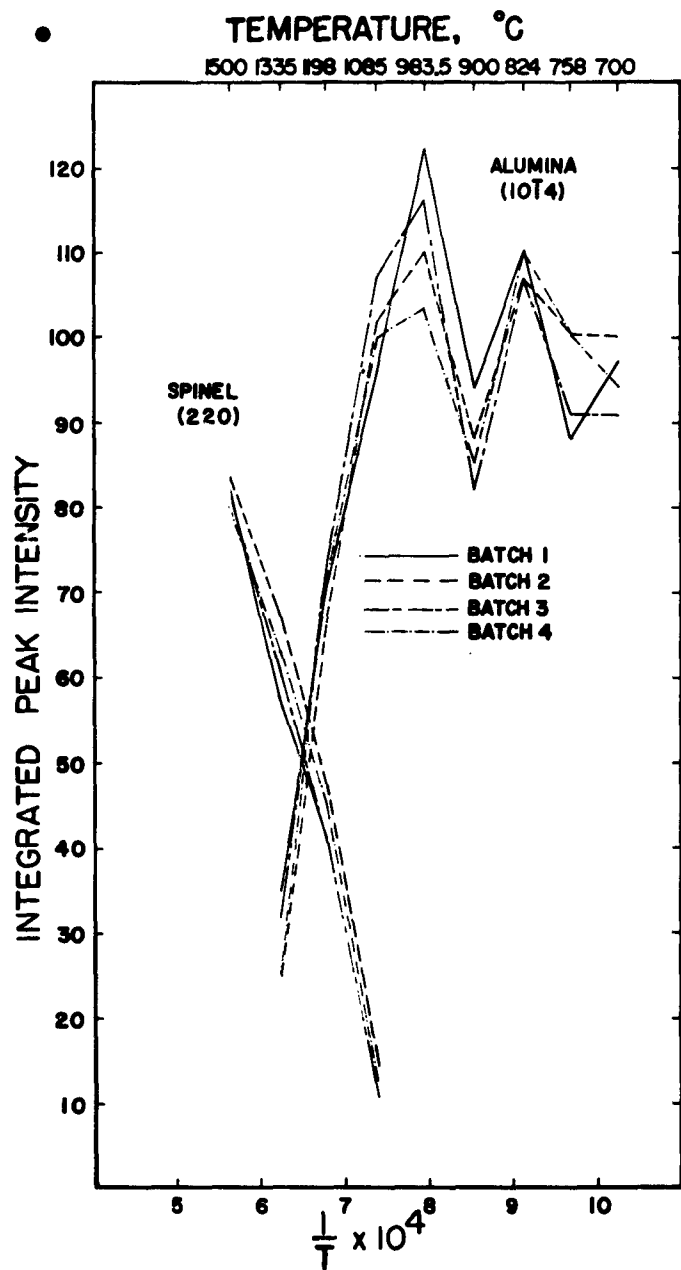


Figure 7. Temperature dependence of x-ray diffraction intensities for mixtures of irradiated and unirradiated alumina and basic magnesium carbonate calcined for 60 minutes.

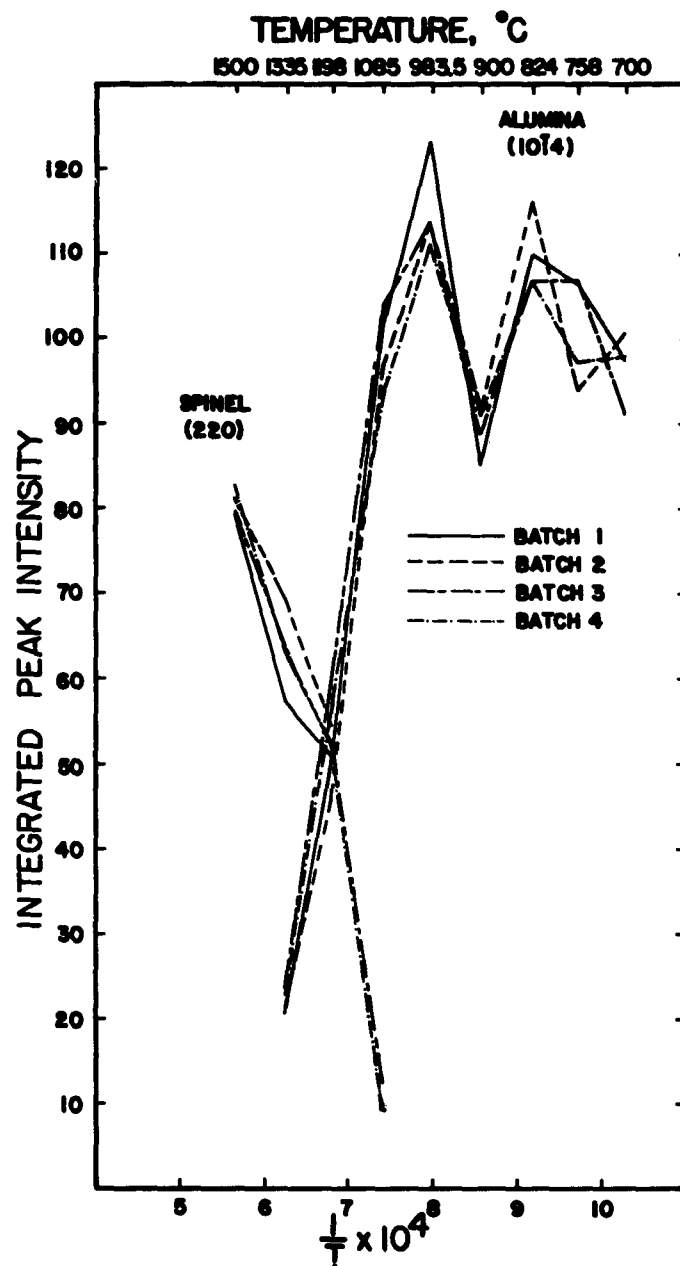
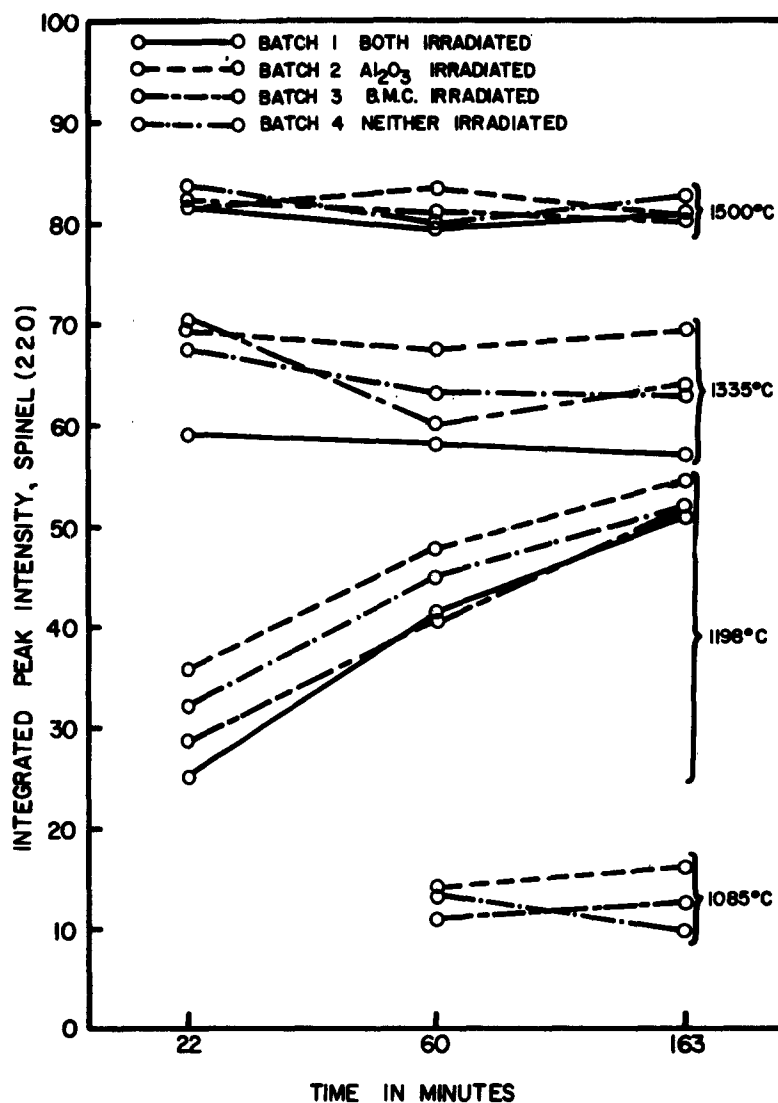


Figure 8. Temperature dependence of x-ray diffraction intensities for mixtures of irradiated and unirradiated alumina and basic magnesium carbonate calcined for 163 minutes.



ISOTHERMAL CONVERSION TO SPINEL AS A FUNCTION OF $\ln(t)$ FOR IRRADIATED AND UNIRRADIATED ALUMINA-BASIC MAGNESIUM CARBONATE MIXTURES.

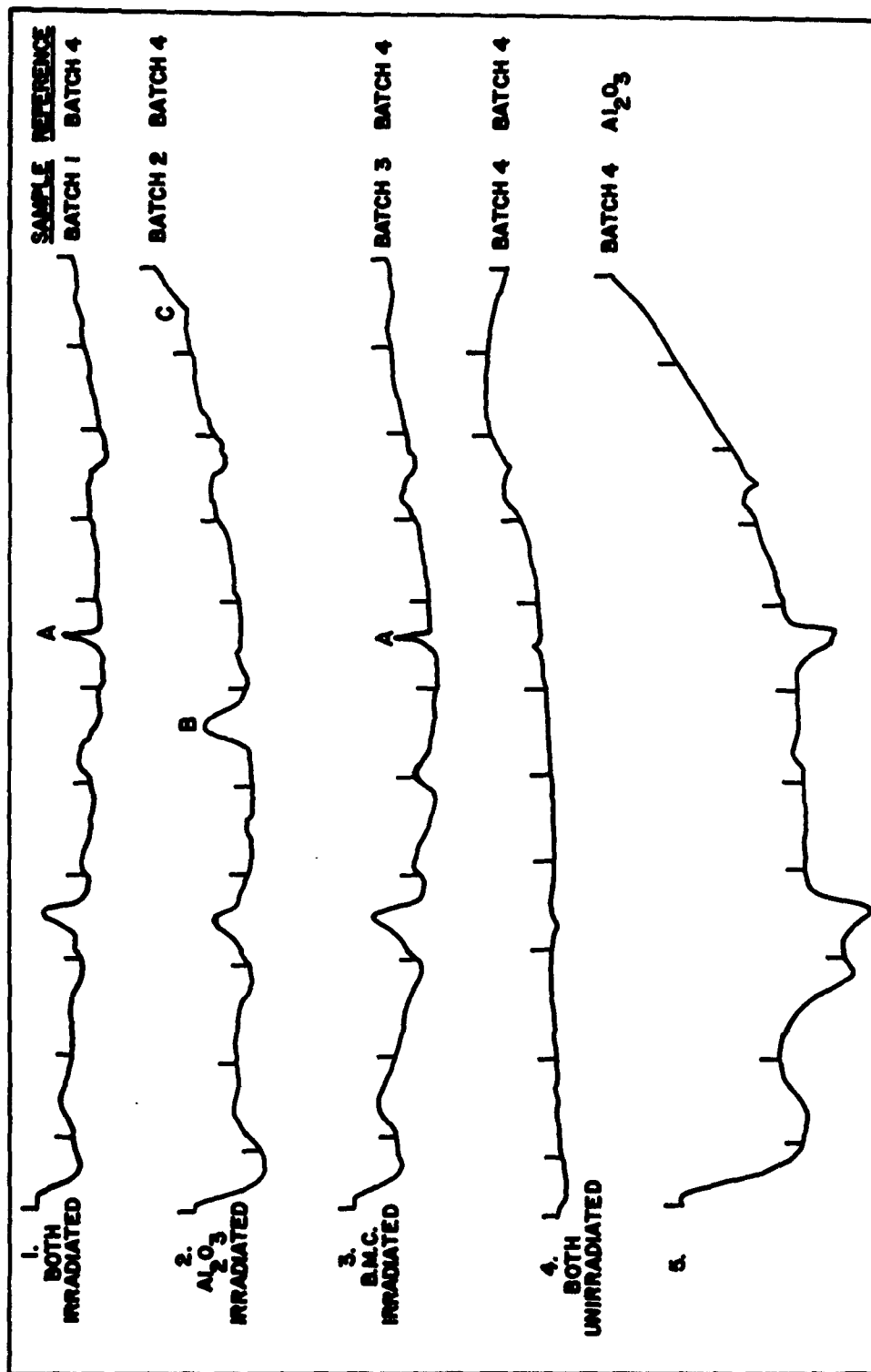
Figure 9. Isothermal conversion to spinel as a function of $\ln(t)$ for irradiated and unirradiated alumina - basic magnesium carbonate mixtures.

for all four batches. It can be seen that at the shortest time (Figs. 6 and 9) spinel is not detected below about 1200°C, but that a gradual decrease in alumina intensity (Fig. 6) begins as low as about 980°C. At longer firing times (Figs. 7 and 8), the same interrelationship between decreasing alumina and increasing spinel intensities is noted, but in these cases spinel formation is detectable as low as 1085°C. At the highest temperature, 1500°C, neither calcination time nor the irradiation history significantly alter the intensity of the spinel peak as is clearly shown in Figure 9. No alumina residue is detected at this temperature and it is apparent that the reaction has been carried essentially to completion, both in terms of the chemical reaction itself and of the degree of crystallization of the spinel product. At lower temperatures, the integrated intensity of spinel is related both to calcination time and to the irradiation history. Batch 2 containing irradiated Al_2O_3 and unirradiated B.M.C. consistently has the highest integrated intensity. Batch 3 containing irradiated B.M.C. with unirradiated Al_2O_3 , and the control, batch 4 (both unirradiated), tend to follow a middle course. Batch 1 containing both species in the irradiated condition generally shows the lowest integrated values (and lowest peak values as well). This apparent anomaly will be discussed later.

Differential Thermal Analyses.⁵ D. T. A. curves of these four raw batches suggest some substantial differences attributable to irradiation which occur in the low temperature range, but such thermal effects due to irradiation are partially obscured by strong endotherms related to the removal of H_2O and CO_2 in the 200°-500°C range. The higher temperature range (to 1350°C) does show that a characteristic broad exotherm relating to spinel formation (and sample shrinkage) reaches its peak at a considerably lower temperature in the case of Batch 2 (Al_2O_3 alone irradiated) than in the other cases. Because of the obscuring low temperature endotherms these curves are not shown. Figure 10 illustrates D. T. A. curves of the same batches which had been precalcined to 700°C in still air for 22 minutes to remove H_2O and CO_2 . To better illustrate differences attributable to the irradiation history, the first four curves were made with Batch 4 (both raw materials unirradiated) serving as the reference material; The fifth one shows the more normal D. T. A. curve of Batch 4 run against an inert Al_2O_3 reference material. The vertical marks on each D. T. A. curve indicate 100°C temperature intervals. All runs were made in flowing oxygen at atmospheric pressure. Three noteworthy events may be seen:

1. The 660°C peak marked (A) in Batches 1 and 3 is not present in Batches 2 and 4. From Curve 5, it may be concluded that this apparent exothermic peak is due to an actual endotherm in the reference material (Batch 4). It is considered to be due to the removal of either water or CO_2 absorbed from the air by MgO

⁵Model DTA-12A, Differential Thermal Analysis Apparatus, a product of the Robert L. Stone Company, Austin, Texas.



DIFFERENTIAL THERMAL ANALYSES OF 700°C PRECALCINED BASIC MAGNESIUM CARBONATE - ALUMINA BATCHES. DYNAMIC PURE OXYGEN, ATMOSPHERIC PRESSURE, 10°C/MIN. RATE, Pt-10% Rn THERMOCOUPLES.

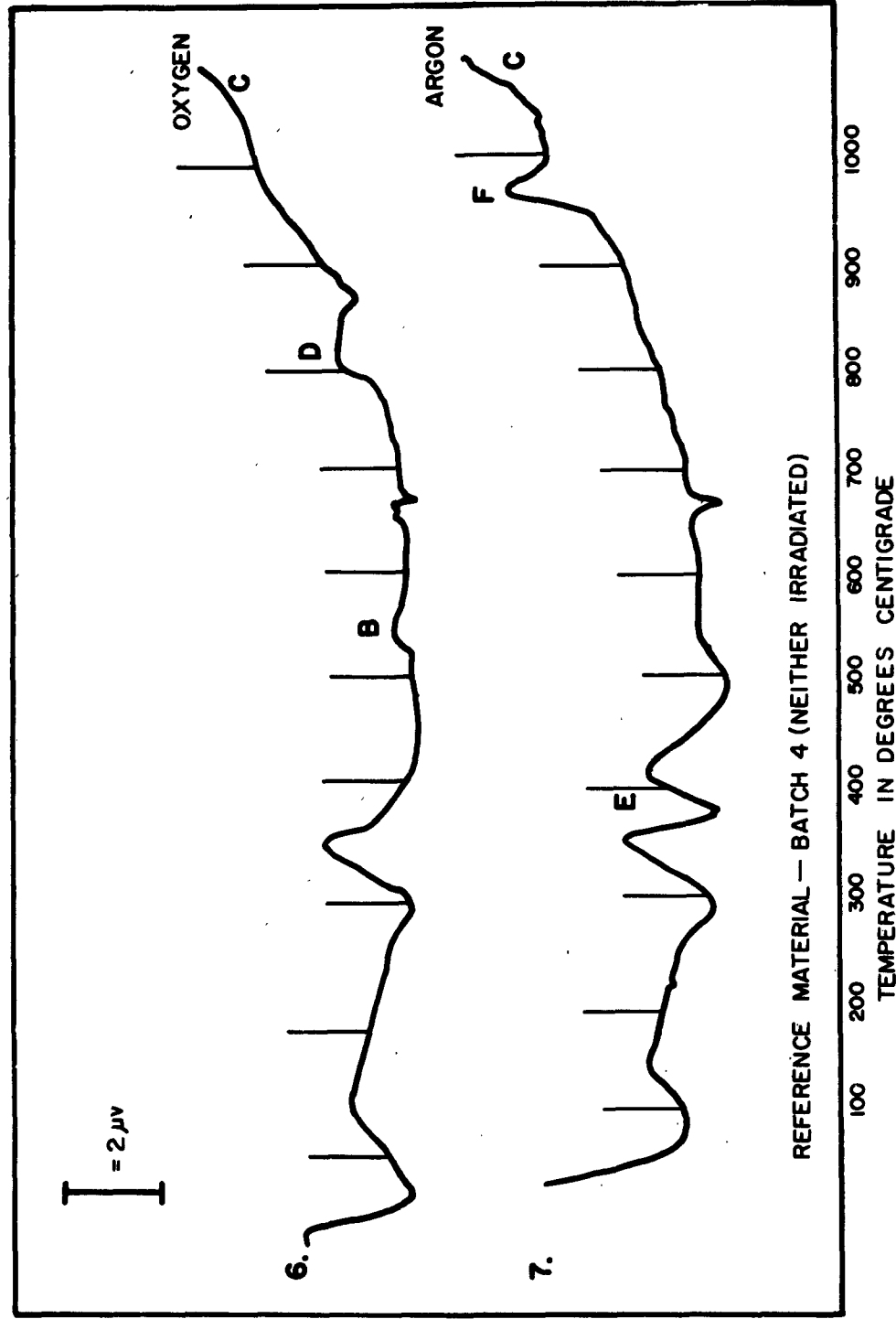
L.D.B.

Figure 10. Differential thermal analyses of 700°C precalcined basic magnesium carbonate - alumina batches. Dynamic pure oxygen, atmospheric pressure, 10°C/min. rate.

(from B.M.C.) after the 700°C precalcination. The fact that this particular endotherm occurring in the reference material was not matched by a corresponding one in the case of the two batches containing irradiated B.M.C. may be cited as evidence that irradiation has indeed altered the subsequent thermochemical behavior of the magnesia material, although the specific changes have not yet been identified.

2. The 565°C exotherm marked (B) in Batch 2 is essentially unique (shows very weakly in Batch 1) and does not correspond to a thermal effect in the reference material (Batch 4).
3. The sharp uptrend in Batch 2 at the point marked (C) corresponds closely in temperature ($\approx 1050^{\circ}\text{C}$) with the initial detection of spinel by X-ray; only Batch 2, containing irradiated alumina alone, shows this exothermic trend as evidence of spinel formation (and more rapid sintering) at so low a temperature. It may be argued that these data lend additional support to the premise that neutron irradiation of alumina, by introducing anion vacancies into the structure in addition to probable cation displacements), might alter the kinetics of subsequent processes which depend on vacancy-controlled bulk diffusion processes. In this light, it is suggested that the exotherm at (B) is related to a release of energy stored in the alumina by irradiation- possibly by "reoxidation" of anion vacancies in this pure O_2 atmosphere- and that the unique uptrend at (C) is due to an enhanced rate of spinel formation attributable to the irradiation of $\alpha\text{-Al}_2\text{O}_3$ - possibly due to a relatively greater abundance of favorable spinel growth sites which were formed over the temperature interval from $\approx 700^{\circ}$ to $\approx 1050^{\circ}\text{C}$.

In order to more clearly delineate the influence of the irradiation of alumina on the spinel reaction, additional differential thermal analyses were run on Batch 2 (irradiated Al_2O_3 and unirradiated B.M.C.) again using the unirradiated Batch 4 as a reference material. As before, the materials were precalcined at 700°C in still air but for 60 rather than 22 minutes as in the previous group. Runs were made in flowing oxygen and in flowing argon at atmospheric pressure. The resulting curves are shown in Figure 11. As would be expected Curve 6 is almost identical to Curve 2 of Figure 10, except that the peak at (B) of Curve 6 is much weaker than in Curve 5 likely due to the longer precalcining time. On the other hand the curve for the sample heated in argon has several notable differences. The cause of the complex at (E) on the argon curve is presently unexplained but appears to be of little moment to this discussion. It is significant that the exothermic peak (B) of Curve 6 (in oxygen) does not appear in Curve 7 (in argon). It is believed that this lack of an exotherm at (B) in an argon atmosphere is valid evidence of a "reoxidation" of the irradiated alumina when it was heated in an oxygen atmosphere. The exothermic peak (F) at about 975°C shown



DIFFERENTIAL THERMAL ANALYSES OF BATCH 2 (Al_2O_3 IRRADIATED) AS A FUNCTION OF DYNAMIC GAS ENVIRONMENT. ALL MATERIALS PRECALCINED AT 700°C, 60 MINUTES.

Figure 11. Differential thermal analyses of Batch 2 (Al_2O_3 irradiated) as a function of dynamic gas environment. All materials precalcined at 700°C, 60 minutes.

in Curve 7 (in argon) is thought to be caused by the release of energy associated with the conversion of the metastable two phase magnesia-alumina mixture to the thermodynamically stable MgAl_2O_4 . In the absence of oxygen the anion vacancies resulting from irradiation would be preserved, maintaining the alumina structure in a higher than normal energy state until a temperature is reached which is sufficiently high for the formation of spinel to begin. Once initiated, spinel formation should proceed quite rapidly, i.e., if the alumina retains anion vacancies up to spinel formation temperatures the augmented mobility of the alumina structure would greatly enhance the rate of spinel formation. This view is strongly supported by the sharp exotherm at F in argon (Curve 7), unmatched in any of the oxygen runs. As a further confirmation of this interpretation, x-ray analyses of the two D. T. A. samples (Curves 6 and 7, Fig. 11) which had been heated to 1100°C (at $10^\circ/\text{min.}$) during the D. T. A. runs showed significantly stronger spinel intensities for the material heated in argon.

The exotherm at (D) on Curve 6 (also Curves 1-4 of Fig. 10) is thought to indicate a phase change in the palladium specimen container associated with the presence of oxygen. It is in no way related to the spinel reaction being studied.

Interpretation of Results

Any interpretation of the experimental results must take into account these points:

1. Irradiation of BMC apparently causes its breakdown at a lower than normal temperature and leaves the MgO residue, after a 700°C precalcination, in a more stable, less reactive state than is normally the case at the temperature at which spinel begins to form;
2. irradiation of $\alpha\text{-Al}_2\text{O}_3$ apparently stores up excess energy within the material, at least some of which is retained after a 700°C still air precalcination, but is released at about 565°C in pure oxygen; and
3. Batch 1, containing both Al_2O_3 and BMC in the irradiated condition, is consistently less reactive under any given time-temperature condition than any of the others, even though it contains the same "active" irradiated Al_2O_3 that presumably accounts for the consistently highest reaction rate (Batch 2).

The contrasts between Batch 1 and Batch 2 may be tentatively explained in terms of the relative cation mobilities in $\alpha\text{-Al}_2\text{O}_3$ and MgO:

- (a) it is generally thought that spinel forms on the alumina surface, and that the reaction rate will be dependent on the diffusion rate of the slower moving cation, probably Al^{+++} ;
- (b) when Al_2O_3 is irradiated, the Al^{+++} mobility should be temporarily increased (at temperatures below which irradiation damage is annealed out), the spinel formation rate should correspondingly increase, as shown by comparing Batch 2 with Batch 4;
- (c) when BMC is irradiated, the metastable MgO residue remaining above $\approx 500^\circ\text{C}$ is apparently in a lower energy state than normal, as evidenced by its lowered sensitivity to rehydration and/or CO_2 adsorption. The effective rate of spinel formation might not be greatly altered, however, since the reaction rate would still be dependent on Al^{+++} mobility in the normal, unirradiated alumina component. This view is borne out by the similarity in x-ray intensities between Batch 3 (BMC irradiated) and Batch 4 (neither component irradiated); and
- (d) when both species are irradiated, interaction effects also must be considered which might either enhance or suppress the effects noted in the cases above. D. T. A. curves of raw batches (not illustrated) show some unusual but as yet unresolved effects for Batch 1 in the $400\text{-}500^\circ\text{C}$ range which are not reflected in the other batches; it is possible (but not proven) that in this case the irradiation-induced damage may be largely dissipated- even in the alumina- at a temperature below the threshold for spinel formation.

Levy (1961) has shown that color center activity in neutron-irradiated Al_2O_3 (sapphire) is destroyed by annealing at temperatures above $\approx 790^\circ\text{C}$, and Choi, et al. (1961) have shown that annealing at 1500°C restores the micro-hardness of irradiated sapphire to its pre-irradiation level. Spinel formation begins $\approx 700^\circ\text{C}$, and is an irreversible process. Spinel formation thus is underway before thermal annealing completely removes the irradiation-induced vacancies. It is probable that the first spinel formed is both widely dispersed and of very small size, i.e., in the early stages this may be considered as a nucleation process. If irradiation enhances spinel formation during this critical stage, producing either larger numbers of spinel nuclei or more stable ones, then more rapid growth rates (as compared with unirradiated material) should continue,

even into temperature ranges where the irradiation-induced mobility can no longer be a factor in further spinel formation. This view seems consistent with these data, and with the basic concepts of reaction sintering.

Summary

The raw material irradiation experiments strongly suggest that anion vacancies (as earlier defined) have a pronounced effect on the rate of spinel formation and that diffusion of the Al^{+++} ions controls the reaction rate in the temperature ranges studied. In view of the rather unexpected and not altogether explained behavior of Batch 1 which was formulated from all irradiated materials, additional quantitative studies are needed. Such experiments using purer materials and more refined techniques are being planned to resolve these anomalies prior to a projected publication of these findings.

VI. CRYSTAL GROWTH

Theoretical Considerations

Theories of the growth of crystals from vapors and solutions have been documented by Verma (1953) and Chalmers (1955). Chalmers also presented a comprehensive treatment of the theoretical aspects of crystal growth from the melt. The review which follows is taken primarily from Chalmers' paper.

Nucleation. The criterion for spontaneous nucleation of a new layer upon a "perfect" layer of atoms is that the density of atoms coming in contact with the surface be sufficient for the probability of the aggregation of a critical sized group of atoms to be high. The factors which affect this probability are:

1. The size of the critical group.
2. The rate of arrival of the atoms at the surface.
3. The average time of stay of an atom between arrival and departure.

From this it is clear that spontaneous surface nucleation should be extremely easy to create in growth from the melt. In crystal growth from the melt the role of the dislocation as a nucleation site can be eliminated; however, if dislocations were present they would be expected to enhance the rate of crystal growth. Even if dislocations are not necessary for crystal growth from the melt, they are invariably found upon examination of the crystal after growth.

Defects. Examination of the crystal after growth shows three types of defects:

1. Vacancies
2. Dislocations
3. Lineages; segments misoriented by less than one degree (also called sub-grain boundaries).

The order of formation of these defects in a crystal grown at a definite rate is believed to be the formation of vacancies (dictated by the thermodynamics of the system) which then coalesce and collapse, forming dislocations, which agglomerate and form the lineage structure. Two other methods by which vacancies can be eliminated in the crystals are the attachment to a dislocation forming a jog and the formation of cavities inside the crystal.

Another mechanism by which dislocations can be formed during growth is one in which stacking faults are involved. A material in which stacking faults are relatively stable thermodynamically will have two possible sites at which the atom will fit. One site corresponds to the stacking fault site. It is obvious that newly deposited atoms will be more likely to adhere to the normal sites rather than the stacking fault sites; nevertheless, the probability is high that some small number of these are formed during growth. Since crystal growth from the melt appears to be a lateral growth of steps, it is possible for the faulted region to become of considerable size. Other layers deposited would perpetuate the error and would produce a region surrounded by a stacking fault. An outward movement of the atoms in the faulted region would produce a disc of vacancies which, upon collapsing, would form a half loop of an edge dislocation.

The mobility of the dislocations in their own slip planes is appreciable in the temperature range necessary for crystal growth, and the dislocations apparently undergo considerable thermal movement since they arrange themselves in stable arrays (lineages) when a sufficient quantity of them have been formed. These arrays are the minimum energy structures that the dislocations can have since dislocations are not thermodynamically stable structures.

Effects of Impurities. In the context of this discussion it should be kept in mind that excess alumina is considered as an impurity in spinel. As would be expected, the impurity nearly always has different solubilities in the solid and the liquid at the same temperature. This difference is usually one of a higher solubility in the liquid form. As a result, a concentration gradient is established during crystal growth; and, consequently, the crystal is not of uniform composition.⁶ This composition gradient, regardless of how small it is, will cause a gradual change in the lattice parameter. Frank (1952) discussed the possibility of the introduction of dislocations by this change in the lattice parameter.

Chalmers (1955) discussed the consequences of the fact that the interface advanced at a temperature below that of the freezing point of the bulk liquid. This occurred because the "pile-up" of the solute ahead of the interface increased the concentration and consequently lowered the melting point in this region. When this happened it was possible for some of the liquid ahead of the interface to be supercooled even though freezing took place readily at the interface without appreciable supercooling. If the extent of this supercooling was limited, then each region that grew in advance of the rest remained thin and many regions were formed. These many regions formed what was called a cellular structure.

⁶This factor should be minimized in the case of flame fusion, since the layer of molten liquid is ideally quite shallow, and is being constantly replenished by feed material of presumably constant composition. See Rudness and Kebler (1960) and Bauer, et al. (1950).

In many cases the formation of this cellular structure resulted in the segregation of the impurities to the walls of the cells. It has been demonstrated by Stewart, et al. (1951) that the cellular structure can be suppressed during growth by maintaining a temperature gradient sufficiently high so that there is no region of overlap.

Brief History of Spinel Crystal Growth

Synthetic spinels have been commercially produced for many years, e.g., in the U. S. A. by the Linde Company, a division of Union Carbide Corporation, and in Germany by the Bitterfeld Works of I. G. Farbenindustrie. Only nonstoichiometric spinels have been marketed, although some scientific laboratories have been able to grow (by various adaptations of the flame fusion process) stoichiometric MgAl_2O_4 boules which broke into small pieces (useful only for some research studies) either during growth or in the subsequent cooling (Rinne, 1928; Jagodzinski and Saalfeld, 1957; Wickersheim and Lefever, 1960). These observations have also been confirmed by Warshaw,⁷ as well as in oxyhydrogen crystal growth experiments carried out to date in this investigation. Lefever⁸ has reported the successful growth and cooling of stoichiometric spinel boules in a flame fusion device by an as yet undisclosed procedure.

The Verneuil Technique

Definition of the Problem. Verneuil (1903) resolved the problem of producing artificial gems⁹ by a flame fusion method to that of satisfying the three following conditions:

1. Maintain the molten product in one constant region of the flame (i.e., at a constant temperature just above the melting point).

⁷Warshaw, Stanley, Raytheon Corporation, Waltham, Mass. Personal communication, 1962.

⁸Lefever, R. A., General Telephone and Electronics Laboratories, Inc., Palo Alto, Calif. Personal communication, 1962.

⁹Verneuil concentrated on ruby and sapphire gems (both $\alpha\text{-Al}_2\text{O}_3$) and, certainly, most of the crystals grown by flame fusion since then have also been of the sapphire type, rather than spinel. It is important to note that, other than the obvious ones due to differences in crystal structure, there are only minor changes in the way these two materials physically respond to the process variables. The differences observed in growth behavior are likely to be of physical-chemical character rather than a direct consequence of the thermal and mechanical parameters of the apparatus. The extensive knowledge of sapphire growth is in general applicable to the case of growing the more complex spinel crystals.

2. Introduce the growth of superposed layers upward in order to realize the refining of a series of shallow layers (i.e., to prevent nucleation of polycrystalline growth).
3. Obtain the fusion within conditions such that the contact of the molten product with the support is reduced to an extremely small surface (i.e., to reduce the growing surface initially to one singly oriented grain).

Original Flame-Fusion Apparatus. To satisfy the first condition Verneuil used a oxyhydrogen blowpipe made of brass, mounted vertically above a refractory support. The refractory support was mounted on a base which could be lowered or raised by a fine-threaded screw so that the crystal could be built up slowly by maintaining the molten product in one constant region of the flame.

A "sifting" process was used to fulfill the second condition. The feed material, fine-grained alumina powder, was placed in a small gauge screen suspended in an oxygen-pressurized chamber connected directly to the center tube of the blowpipe, and was fed into the oxygen stream and thus into the flame by the vibratory action of a small mechanically-activated hammer which periodically tapped the rod supporting the screen. The fine alumina particles were thus distributed in all parts of the flame where they became molten upon reaching the portion of the flame which is hot enough to melt the alumina ($\approx 2040^{\circ}\text{C}$).

Verneuil met the third condition by heating the refractory support to a temperature slightly below the melting point for alumina, such that only the grains which fell on the refractory tip agglomerated to form a cone which grew until it finally reached a portion of the flame hot enough to melt the tip of the cone. At this point the boule began to grow, and all the particles of feed material falling on it were molten.

The diameter of the boule was then increased in proportion as it reached a hotter and larger zone of the flame. When a spherical shape was achieved, the diameter of the boule was then increased by progressively increasing the oxygen flow. Since the hydrogen was admitted in excess at the beginning of fusion, the increase in the flow of oxygen displaced the proper zone of fusion making it necessary to move the support (carrying the growing boule) to properly maintain its molten top within the zone of fusion. When the boule had achieved a size of 12 to 15 carats, Verneuil quickly shut off the gases, quenching the boule.

Verneuil's perceptive analysis of the problems involved, and his solution of them in terms of apparatus and procedure, and the more recent and very detailed analysis of Russian crystal growth technology (Popov, 1959) stand as major landmarks in the literature of the practical art of crystal growth by flame fusion.

Analysis of Limitations. For sixty years, the Verneuil method has been used extensively in experimental and commercial crystal growing practice. Other than

mechanical modifications directed at means of producing a more uniform feed of material, automating for efficient production, or increasing the size of crystals produced, there have been but few significant technical improvements in the basic flame fusion apparatus. Thus present day commercial crystals of sapphire or spinel do not differ greatly in terms of purity and freedom from structural defects from those which were (or could have been) grown with Verneuil's original equipment.

The traditional apparatus employed for flame fusion crystal growth is open to criticism in terms of its contributions to the impurities and imperfections of its product on at least three counts:

1. It serves as a source of cation impurities, particularly those abraded, oxidized, or scaled from its metallic components; such impurities are likely to be kept "active" within the hot wall furnace where vapor transport is a significant factor.
2. It usually operates in a cyclic (and hence inconstant) fashion, in which a pulsed flow of feed material (caused by the tapping device) periodically alters not only the temperature and thickness of the melt at the growth face, but also the flame conditions and the heat transfer conditions within the furnace. The combined action of these rapidly varying conditions is thought to make a significant contribution to the high population and erratic distribution of various crystalline defects found in such crystals (Palmour and Kriegel, 1961; Sheuplein and Gibbs, 1960).
3. It generates an "active" atmosphere, one which ideally contains only water vapor, but almost always containing either excess oxygen or hydrogen. Thus the flame atmosphere must be regarded as an active source of anion impurities; H_2O or OH^- has been detected by infrared spectroscopy in flame-grown spinel crystals (Wickersheim and Lefever, 1960).

Recent Modifications of the Verneuil Method. Three significant modifications of the Verneuil technique dealing specifically with the last of the three problems outlined above, i.e., the atmosphere, have evolved in recent years. The tri-cone ($O_2-H_2-O_2$) burner (See Bauer et al., 1950; Lefever and Clark, 1962) provided for more efficient combustion and a better range of controlled flame stoichiometry, making practical the growth of single crystals of rutile (TiO_2) and other easily reduced oxides. Lefever and Clark (1962) recently have developed a three-gas torch ($O_2-H_2-O_2$) of quite different design which is reported to yield even higher working temperatures and a uniform, sharply oxidizing flame.

De La Rue and Halden (1960) introduced a flameless form of the Verneuil process in which heat was supplied to the growing crystal by arc-imaging techniques. The growing crystal was completely isolated within a transparent glass envelope, i.e.,

a cold wall furnace, and any atmospheric environment could be selected. Unfortunately, the crystals of sapphire and spinel of interest in this investigation are highly transparent to infrared, and thus cannot be readily melted by the arc-imaging method.

The invention of the R. F. plasma torch of Reed (1961a, 1961b, 1962) has opened up still wider possibilities for crystal growth, since any material can be melted and vaporized within its $\approx 15,000^\circ\text{C}$ plasma "flame." Although other plasma sources had been employed somewhat earlier for growth of refractory metal and oxide crystals (other plasma sources have been reviewed by Field, 1961 and Field and Bauer, 1961), Reed's R. F. plasma appears uniquely suited for oxide crystal work in being electrodeless, effectively noncontaminating, and capable of operating at very high temperatures over a wide range of atmospheric conditions, including oxidizing ones.

Alternative Methods

Possible alternatives to flame fusion in its various modifications as a means of growing spinel single crystals include the hydrothermal technique of Laudise and Ballman (1958) and the "pulling" of a crystal from the melt by the Czochralski (1917) technique. Laudise and Ballman found that for the systems $\text{NaOH-H}_2\text{O-Al}_2\text{O}_3$ and $\text{Na}_2\text{CO}_3\text{-H}_2\text{O-Al}_2\text{O}_3$ pressures generally in excess of 30,000 psi and temperatures of the order of 4300°C were required for the synthesis of sapphire. The growth rates were low (0.002 to 0.010 inches per day) and high levels of impurities (of sodium and container materials) seemed certain. Applications of the Czochralski technique to the spinel case appear to be limited by the requirement for an electrically conductive and refractory crucible capable of operating in an oxidizing atmosphere at temperatures above 2000°C while remaining inert to molten spinel.

Experimental Equipment

The shortcomings of the traditional Verneuil furnace for the growing of acceptable crystals for research purposes have been stated in an earlier section, i.e., (1) introduction or recirculation of cation impurities, (2) erratic or pulsating material flow and (3) an unavoidable "active" atmosphere. In order to overcome these objections two new crystal furnaces have been designed for use in the experimental phases of this program. The first, an oxyhydrogen crystal grower, was designed to investigate means of overcoming the first two sources of difficulty and the second, an R. F. plasma crystal grower, has the possibility of overcoming all three.

Oxyhydrogen Crystal Grower. For the research purposes intended here, the design and construction of the first crystal grower has been a straightforward matter, except for the three most critical components, i.e., the feed handling

system, the torch, and the furnace. These units and some specific objectives inherent in their design are summarized below.

A device for smoothly introducing feed material was developed based on a small Syntron vibratory parts feeder.¹⁰ The drive unit, mounted in an inverted position on the lid of a pressurized aluminum conical hopper, energizes a modified Syntron helical feed bowl suspended on an extension shaft within the pressurized hopper, as illustrated in Figure 12. It continuously feeds material, at an easily adjusted rate, up the helical groove from the central "reservoir" of the Syntron bowl to the exit gates at the lip, from which the fine particles drop into the oxygen stream, moving through the torch and thence to the growing crystal. This feed system was developed with two specific objectives in mind. The first was to provide an electro-mechanical handling system which would not contribute cation contaminants to the feed material through abrasive action. As the criteria for materials purity advance to more stringent levels in this program, such a system can be "cleaned up" in at least two ways, i.e., by making the components from, or coating them with, non-contaminating metal of ultra-high purity (99.5 + % aluminum in the present unit) or by coating interior surfaces with a low-friction, wear-resistant and non-contaminating surfacing material like Teflon (the procedure being followed in the feeder for the R. F. plasma unit now under construction). The second objective, continuous feeding over a wide range of feed rates, is predicated on the view that the intermittent feed traditionally used in commercial crystal growing operations is partially responsible for many of the defects found in commercial single crystals. In commercial operations sporadic feeding is probably warranted due to the increase in the rate of growth which may be achieved. However, for research studies, where crystals having a minimum of random growth defects are necessary if statistically valid data on structure-sensitive properties are to be obtained, a smooth and continuous flow of clean feed material to the crystal is regarded as a necessary experimental condition.

Oxygen (bearing the feed material) moves downward from the feeder through a Swagelok-sealed, semi-rigid plastic tube extending into the torch almost to the burner tip, as illustrated in Figure 13. The axially drilled aluminum torch body serves as an extension of the oxygen feedpipe and is fitted with interchangeable high purity alumina torch tips of different bore sizes. The hydrogen fuel is introduced from the upper plenum chamber through eight drilled passages into the lower plenum chamber, and thence through an orifice-adjusting sleeve threaded onto the torch body, finally mixing with oxygen within and beyond the high purity alumina torch nozzle. Adjustment of the sleeve alters the hydrogen velocity for a given flow rate as a function of the spacing of the annular orifice at the 60°-tapered "needle valve" section between the concentrically ground alumina nozzle

¹⁰Model EB-00, a product of the Syntron Company, Homer City, Pennsylvania.

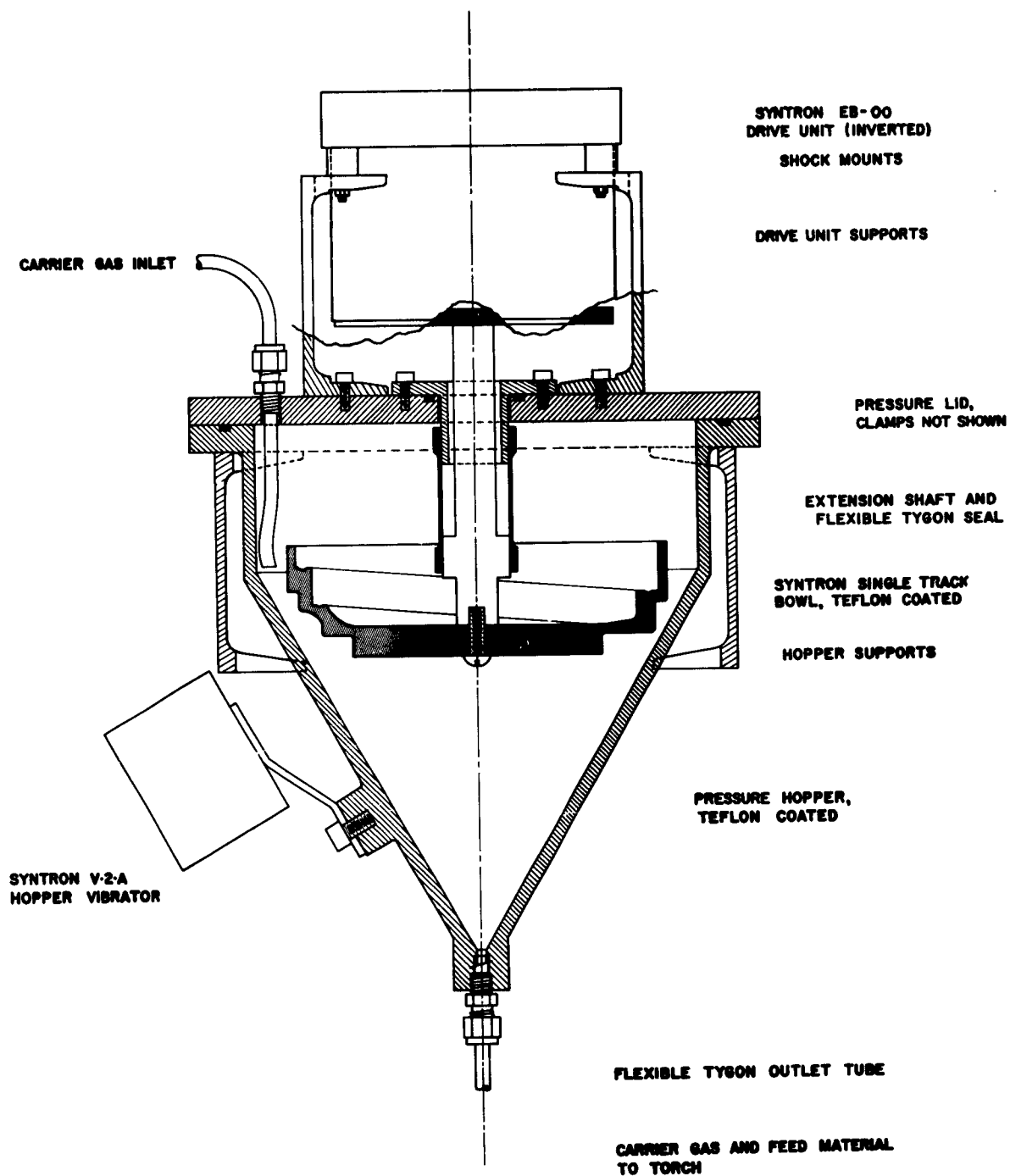


Figure 12. Pressurised material feeder for crystal growth.

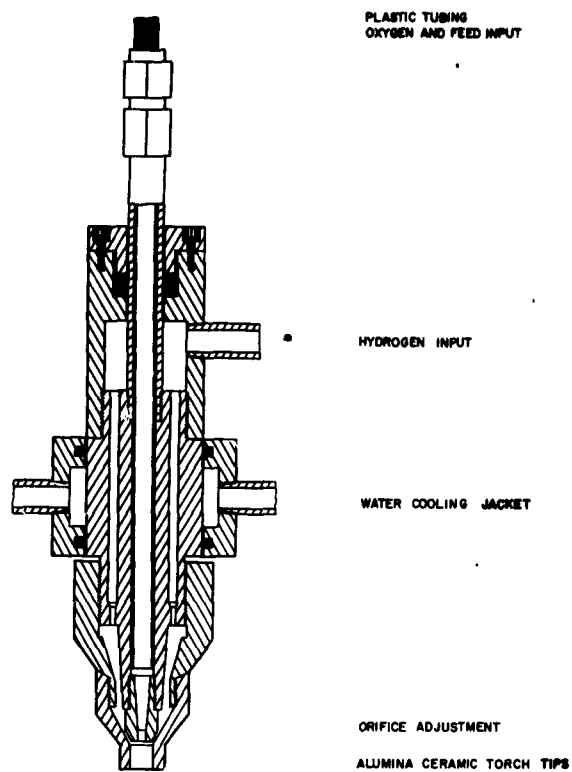


Figure 13. Arrangement for crystal growing with the oxyhydrogen heat source.

and tip¹¹ so that the degree of turbulent mixing of hydrogen and oxygen may be selectively controlled. The torch body is fitted with an "O" ring-sealed water jacket to dissipate heat picked up by the torch from the combustion gases, the hot furnace, and the growing crystal.

Control of the heat output, flame pattern, and flame stoichiometry can be established in these ways: (a) flow rates of oxygen and hydrogen may be varied over wide limits, altering both heat flux and flame stoichiometry, while maintaining a stable flame and a controlled flow of feed material, (b) the orifice may be adjusted to alter the mixing of the combustion gases, thereby changing the relative size and height of the effective crystal-growing zone, and (c) the alumina ceramic nozzles and tips having different bore diameters may be exchanged to alter the flame cross section and the maximum available heat flux.

The apparatus incorporates two furnace options. A conventional hot-wall furnace constructed from insulating alumina brick has been employed in much of the work to date. This furnace, pictured in Figure 14, has a 1.5 inch bore and most favorable growth conditions in it have been obtained when the molten growth face is about seven inches below the torch nozzle. The furnace and its supports are normally wrapped with insulating multiple layers of heavy duty aluminum foil to eliminate stray drafts and pickup of oxidized and vaporized impurities. This figure also illustrates several other parts of the apparatus including the feeder; the torch; gas, water and electrical controls; and the crystal rotator and withdrawing mechanism.

One means of improving the purity of a growing crystal is to lower the vapor pressure of gas-borne extraneous impurities. This approach has been investigated with a cold wall furnace for the crystal grower, following the principle that a cold surface will trap rather than emit unwanted impurities. This water cooled furnace with a two inch bore, illustrated in Figure 15, is constructed of aluminum in a double walled configuration. It is so efficient in terms of heat transfer that condensation will occur on its inner wall less than one inch away from an incandescent growing crystal unless hot water is used as the coolant.

R. F. Plasma Crystal Grower.¹² Later phases of this investigation will make extensive use of an R. F. plasma crystal grower. This unit, designed in this first phase and now under construction, embodies the essential features of Reed's

¹¹The nozzle and tip, as well as the seed candles, are fabricated to precise tolerances from AP-35 (99%) alumina ceramic, a product of the McDanel Refractory Porcelain Co., Beaver Falls, Pa.

¹²A special acknowledgement is due Dr. Thomas B. Reed, Lincoln Laboratories of M. I. T., Lexington, Mass., for illuminating discussions and most helpful advice concerning the R. F. plasma torch and its operation.

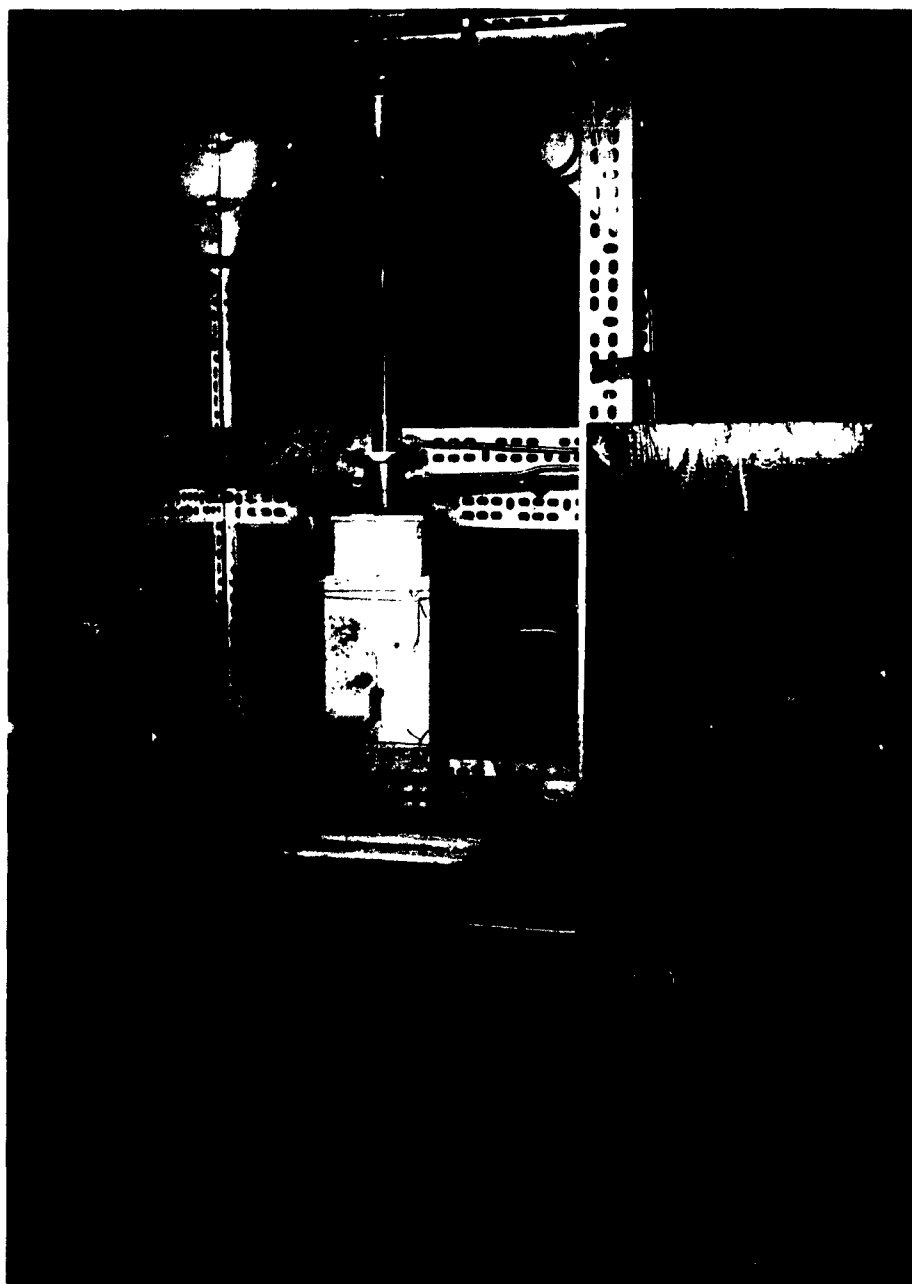


Figure 11. Oxyhydrogen crystal growing apparatus with alumina hot-wall furnace.



Figure 15. Cold-wall furnace for oxyhydrogen crystal grower.

R. F. plasma torch, along with feed handling and crystal handling mechanisms which are second-generation devices derived from those already in use on the oxyhydrogen apparatus. The plasma torch, the load coil, and the approximate position of the growing crystal are illustrated in Figure 16. The plasma fireball generated by the R. F. field (≈ 4 mc) is positioned within and below the plane of the load coil concentrator, and creates a long tail flame in which extends axially for some distance below the torch. The plasma is sustained by argon (which may contain admixtures of other gases) entering at input 2 and flowing down the inner annulus. The plasma is constricted, shaped, and kept away from the fused silica tube walls by additional argon (introduced at input 1) flowing with a swirling motion down the narrow outer annulus. Feed material suspended in a carrier gas (argon or argon-active gas mixture) is injected into the plasma by means of the small-bore central tube (input 3). Figure 17 shows the partially completed crystal grower and its 2.5-5 mc, 10 Kva saturable reactor-controlled power supply. The crystal grower includes gas controls at the top, electrical and mechanical controls immediately below the front viewport, and cooling water controls on the lower access panel. Water-cooled panels equipped with front and side viewports enclose the entire "hot zone" as protection against the intense light, heat, and electrical hazards of the plasma. Portions of the crystal handling mechanism (providing rotation, translation, and withdrawal) may be seen inside the lower part of the structure.

Experimental Procedures

More than a year's cumulative experience with the oxyhydrogen crystal grower has served to work out apparatus difficulties, to evaluate materials and components, and above all, to develop skill and judgement on the part of the operators. Much of this exploratory work has been done with sapphire rather than spinel, partly because the sapphire is somewhat easier to grow, and partly because good feed material and appropriate seed crystals have been more readily available and far less costly. The procedures summarized in this section have been developed to the point where excellent whole sapphire boules of water-white quality can be produced in any desired orientation in the hot wall furnace, and where good alumina-rich spinel boules can be grown, although not so easily or so reliably. While satisfactory progress has been made toward growing good crystals in the cold wall furnace, and toward growing spinel crystals which more nearly approach stoichiometry, these more difficult tasks (requiring special materials and/or modified procedures as well as overall proficiency and judgement in crystal growing methods) have been deferred until other supporting phases of the program are developed more fully.

Review of Control Variables and Growth Parameters. In crystal growth, there is much interaction between variables, and most of the important parameters are difficult to measure other than by indirect means. Consequently it is well to preface the summary of procedures with a brief review of the available controls



Figure 16. Arrangement for crystal growing with the R. F. plasma heat source.

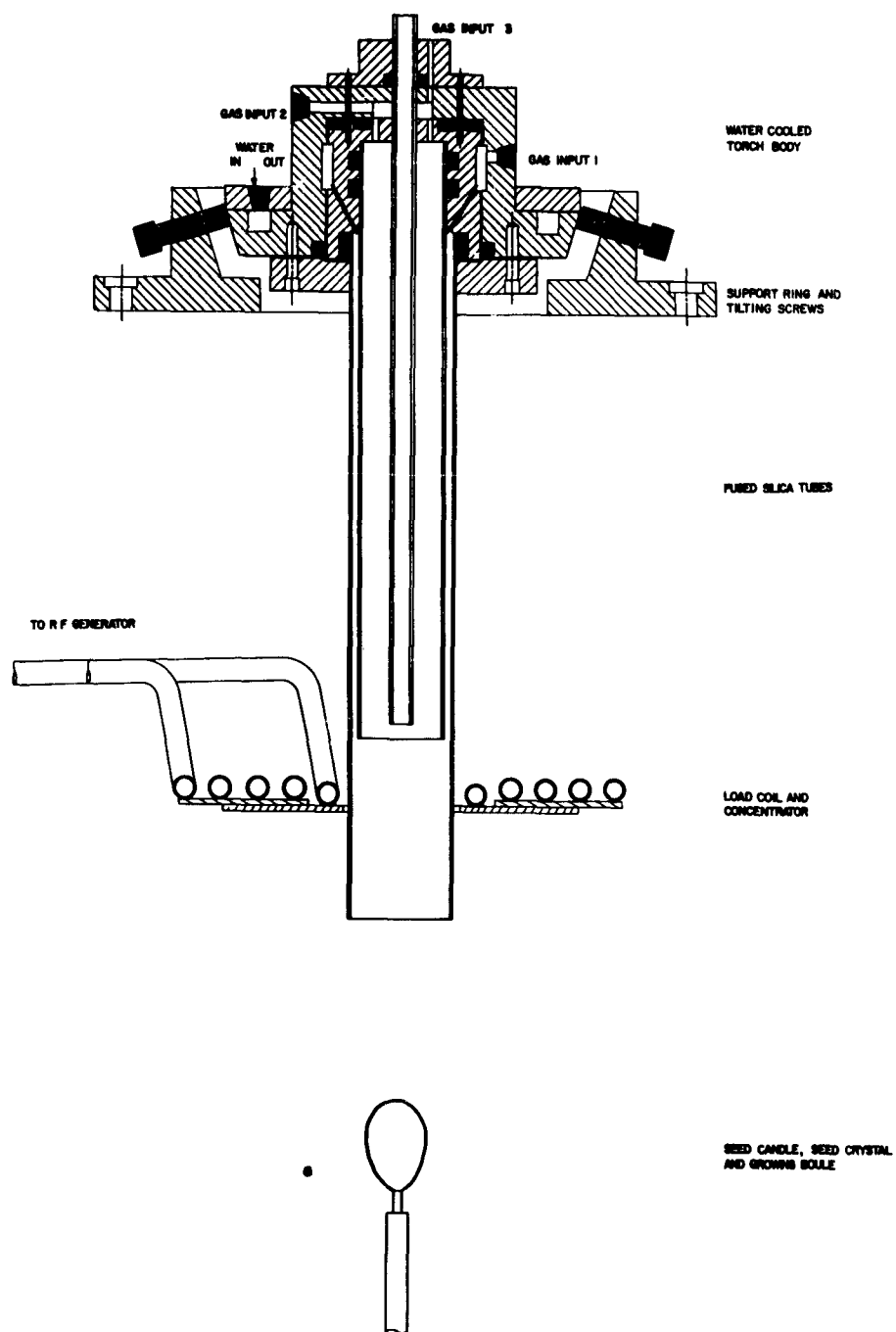


Figure 17. R. F. plasma crystal grower under construction.

(called experimental variables) and the significant conditions (called parameters) which govern growth behavior. The operator has control over these independent experimental variables:

Oxygen flow rate	(variable over wide range)
Hydrogen flow rate	(variable over wide range)
Material feed rate	(variable over wide range)
Crystal withdrawal rate	(variable over wide range)
Rotation of crystal	(off-on only, 9 rpm)
Position of growing boule	(manual control)

The "true" parameters in the system, however, probably are these:

- Heat flux
- Flame stoichiometry
- Flame velocity and uniformity
- Temperature and temperature distribution
- Boule size and shape
- Material feed rate
- Withdrawal rate

Of these, only the latter two bear any simple relationship to the control variables.

These several parameters first must be sensed from the appearance of the flame, the shape and clarity of the melt, and the shape, size, clarity, and surface texture of the growing boule. Then they must be resolved in terms of proper combinations of the experimental variables so that effective regulation can be achieved.

Loading and Aligning. Prior to light-off of the oxyhydrogen crystal grower, a number of preliminary steps must be taken. Material must be placed within the feeder bowl, and the hopper closed and sealed. Oxygen and hydrogen sufficient for an entire run (normally lasting 2-3 hours) must be available at the manifolds and the delivery pressures must be adjusted to agree with flowmeter calibration pressures (seven psi for H_2 , ten psi for O_2). An appropriate seed crystal must be

fitted into the seed candle (a 10 inch long alumina rod precision ground to achieve concentricity of rotation and drilled to accept 0.090 inch diameter seed crystals (see footnote 11). Best results have been obtained with seed crystals which project about 2 cm. above the candle. Such crystals do not neck down too severely, the temperature at the top of the candle remains low enough so that polycrystalline growths do not form there and climb to interfere with the boule, and the seed crystal usually does not weld to the candle. The seed-candle assembly must be aligned in the chuck of the crystal rotator so that concentricity within about 0.005 in. TIR is achieved at the tip of the seed. Obviously, there must be almost perfect axial alignment between flame, seed crystal, and furnace bore.

Lighting and Warmup. An alcohol-soaked Fiberfrax wick on a wire extension handle is inserted in the furnace viewport to light the torch while hydrogen is flowing at a moderate rate. Oxygen is then gradually introduced to obtain a long, smooth-burning flame which is slightly hydrogen-rich ($H_2 = 11$ liters/min; $O_2 = 5$ liters/min.). The seed and candle are then slowly raised to a level about 8 inches below the torch, and after about 15 minutes the refractories attain thermal equilibrium at a temperature somewhat below that required for melting and growth, and the flame is quite stable.

Initiating and Maintaining Growth. Following warmup, the gas flow rate is increased ($H_2 = 16.8$ liters/min.; $O_2 = 7.9$ liters/min.) to attain normal growth conditions, and the seed is gradually raised until its tip fuses to form a clear rounded melt. The melt is maintained at this level (about 7 inches below the torch in the hot wall furnace, and about 6 inches in the cold wall unit) throughout the growth process.

With the tip of the seed crystal molten, and with the candle and seed rotating, material feed is begun, slowly at first. An essentially continuous flow of very fine particles- small enough to melt before landing on the fused top of the growing crystal -is required to increase the size of the melt.¹³ As the diameter of the crystal is increased, heavier feed rates are required, and cooperative adjustments of feed and withdrawal rates are necessary to maintain a properly shaped, clear melt at the optimum height with respect to the torch (Popov, 1959, has analysed in some detail the various shape factors and visual defects of growing crystals in terms of the process variables responsible for them).

¹³Clear melts and good growing conditions have only been achieved in hydrogen-rich flames. In part this may reflect incomplete mixing, and hence a stoichiometry gradient through the flame cross-section. However, it has been such a characteristic feature under all experimental conditions that one tends to conclude that an anion deficiency enhances growth.

The formation of polycrystalline growths occurring either at the actual growth face or along the sides of the boule may be the result of any one of these factors: material feed rate too high; uneven feed deposits; poor alignment; or rapid temperature changes due either to vertical displacements of the boule or to changes in heat flux. Polycrystalline material inhibits or totally precludes further single crystal growth if it occurs on the growth face, and polycrystalline growths along the sides frequently serve as focal points for the initiation of fractures during cooling. In general, the diameter of the growing boule must continue to expand (even though at a very slow rate) to avoid negative slopes upon which polycrystalline growth is almost certain to occur. Sapphire crystals can be grown with essentially straight sides under favorable conditions, but a definite positive slope seems almost essential in the case of spinel.

Quench Cooling. Whole boules of sapphire containing no fractures and few x-ray evidences of strain have been obtained by a quench cooling procedure, whereas those annealed slowly have almost always sustained some fracture damage. It should be pointed out that the annealing experiments to date have been manually -and fairly crudely- controlled, so that momentarily high thermal gradients could have occurred.

Termination of a run by quench cooling in the hot wall furnace includes these steps:

- (a) the flow of feed material is stopped and the crystal is allowed to equilibrate with the flame still operating under full growth conditions;
- (b) during this brief period the viewport is completely closed with Fiberfrax, and Fiberfrax is progressively placed around the furnace base until only a small exit for the exhaust gases remains;
- (c) then withdrawal and rotation are stopped, the oxygen and hydrogen are simultaneously cut off, and the furnace exit is quickly and completely plugged with Fiberfrax so that the crystal is protected from chilling drafts and the furnace heat is conserved. Under these conditions the boule will cool safely in about one hour.

VII. EFFECT OF ATMOSPHERE ON PRECIPITATION HARDENING IN ALUMINA-RICH SPINEL

One of the early experimental phases of this study involved the determination of the azimuthal dependence of Knoop microhardness (Knoop, et al., 1939), and microbrittleness, on one (100) plane of alumina-rich spinel. Figure 18 clearly illustrates the inverse relationship between microhardness and microbrittleness, and the rather asymmetric character of the response (only partly due to tilt between the actual surface and the true (100) plane) which have been previously noted in this laboratory in similar microindentation studies of sapphire. Although there are local variations in behavior, both microhardness and microbrittleness tend to be at minima in the $\langle 110 \rangle$ directions, coinciding with traces of $\langle 110 \rangle$ Burgers vectors for slip on $\{111\}$ planes. These findings are in general agreement with those reported for spinel by Kronberg (1960) and Hornstra (1960, 1962) and also are comparable with data for azimuthal dependence in sapphire obtained by Palmour and Kriegel (1961) and Choi, et al. (1961).

Interrelationships between several of the parameters already outlined have been examined in a thesis by McBrayer (1962) from which the following is abstracted:

Alumina-rich magnesium aluminate spinel single crystals may be hardened by proper heat treatment which may be detected by Knoop microhardness measurements. The change in microhardness in the $[110]$ and $[112]$ directions on the (111) plane have been separately expressed in the form of multiple quadratic regressions in terms of $1/T$, $\ln t$, and \ln percent oxygen over the range 700-1400°C, 5-1200 minutes, and 1-50% O_2 respectively. The regressions show an annealing of the spinel in the temperature range 700-900°C followed by an increase in the hardness in the temperature range 900-1400°C. This rehardening phenomenon appears to result from the formation and subsequent growth of α -alumina nuclei.

This increase in hardness may be retarded by increasing the oxygen partial pressure and is attributed to a decrease in the number of available oxygen vacancies in the spinel lattice. The large, closely-packed and relatively sluggish oxygen ions may be considered as the rate-controlling ions in material transport processes in spinel. A net decrease in anion vacancies must bring about a consequent slowing-down of diffusion-controlled processes in spinel such as the exsolution of α -alumina.

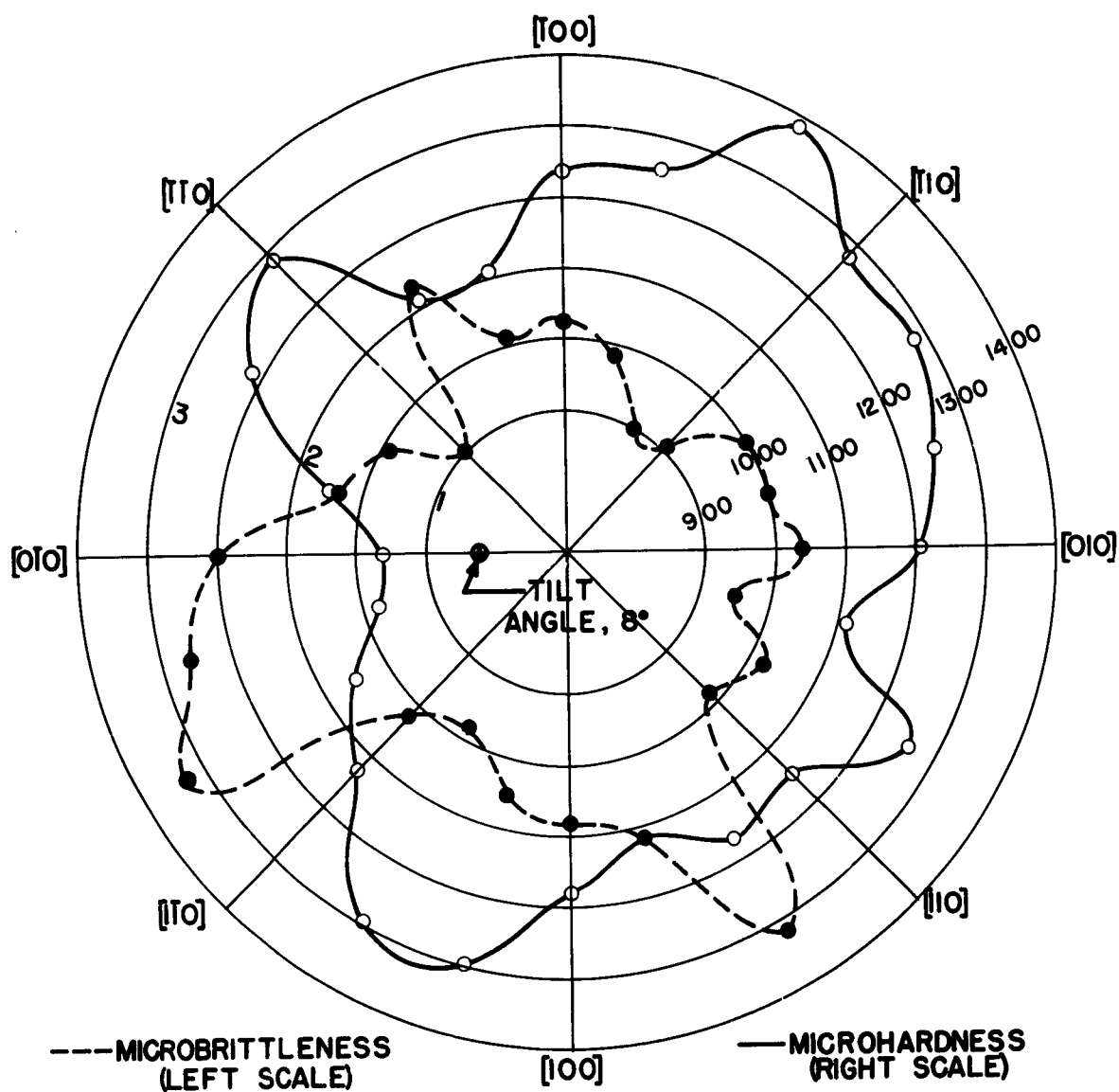


Figure 18. Azimuth dependence of microindentation behavior on (001) of Linde synthetic spinel rod, as-polished. Each point is average of 10 Knoop indentations (100g), 0.003" apart along the radius, long axis normal to indicated direction.

Previous investigators reported a hardening phenomenon at lower temperature which was attributed to the formation of an intermediate phase. This intermediate phase did not appear in this investigation. Whether the absence of the intermediate phase is due to a relatively low $\text{Al}_2\text{O}_3:\text{MgO}$ ratio or a low level of impurities was not established.

These findings,¹⁴ to be the subject of a subsequent technical publication, are considered encouraging in that the apparently hitherto unreported atmosphere dependence, influencing both structure and physical properties, clearly intimates that atmosphere must be considered as a real variable in both growth and deformation processes. In this light, the problem encountered in growing stoichiometric crystals by the Verneuil oxyhydrogen method may be thought of as being due to an unfavorable reaction between the growing crystal and the active water vapor-hydrogen atmosphere, becoming more pronounced as the MgO content of the spinel is increased toward 1:1 stoichiometry. If this is the case, then the problem may be related to a process variable specific to the oxyhydrogen flame fusion crystal growth technique, and not to an inherent instability of 1:1 spinel itself (note that polycrystalline stoichiometric spinel is "well-behaved" and extremely stable). The wide latitude of oxidizing, neutral, and reducing atmospheres independently available in the R. F. plasma crystal grower now under construction will shortly provide an opportunity to test this hypothesis.

¹⁴Based on detailed study of more than 20 like-oriented specimens cut from a single boule grown from Linde AP-393 (3.5:1) spinel boule powder in the oxyhydrogen furnace by the procedures described in Section VI.

VIII. SUMMARY

Most of the work discussed in Sections II through VI has been directed at the various problems associated with growing spinel crystals. Some of these phases are well advanced, others less so. In general, progress toward the attainment of those overall project objectives relating to crystal growth is considered quite satisfactory. Recent successes in the development of dislocation etch pit techniques for spinel (to be described in a future report) and the availability of new and/or improved analytical facilities, including emission spectroscopy for determinations of trace impurities; ultraviolet, visible, and infrared spectroscopy for optical absorption studies of color centers, etc; and high temperature x-ray and high temperature microscopy for structure studies considerably enhance the prospects for effective treatment of the remaining problems concerned with growth and the characterization of growth-related defects during coming months.

Only a few crystals really suitable for deformation studies have been available either from commercial sources or from the early crystal growth experiments described above. The microindentation experiments briefly outlined in Section VII thus constitute the first systematic investigations of interrelationships between deformation, structure, and environment to be undertaken in this program. The prospects for future experimentation in strength and deformation studies have been considerably enhanced by the physical testing experience already gained on a related project concerned with polycrystalline spinel (Contract DA-01-009-ORD-903), and by the installation of a new high temperature (to 2500°C) testing facility for the Instron physical testing machine.

On the basis of these studies still in progress, it is inappropriate to attempt to reach definitive conclusions. There are, for example, implications throughout this report that atmospheric environment may be a strong factor in both growth and deformation processes and that this factor in effect operates by creating an anion-deficient structural state in spinel. But such evidence, although interesting and thought provoking in regard to further experiments, must still be regarded as circumstantial until additional proofs can be obtained.

APPENDIX A

STRUCTURE AND PHYSICAL PROPERTY

DATA FOR SPINEL

Formal Specification of the Spinel Structure

Space Group. O_h^7 - $Fd\bar{3}m$ (Bragg, 1915; Mishikawa, 1915; International Tables of X-ray Crystallography, 1952).

Atomic Positions. (Ewald and Herman, 1926).

8-fold position: 8 metal ions in (a), 000, $1/4$ $1/4$ $1/4$.

16-fold position: 16 metal ions in (d), $5/8$ $5/8$ $5/8$;
 $5/8$ $7/8$ $7/8$; $7/8$ $5/8$ $7/8$; $7/8$ $7/8$ $5/8$.

32-fold position: 32 oxygen ions in (e), $uu\bar{u}$; $u\bar{u}\bar{u}$; $1/4-u$,
 $1/4-u$, $1/4-u$; $1/4-u$, $1/4+u$; $u\bar{u}\bar{u}$; $1/4+u$;
 $1/4+u$, $1/4+u$, $1/4-u$.

With translations: $+(000, 0 \ 1/2 \ 1/2, 1/2 \ 0 \ 1/2, 1/2 \ 1/2 \ 0)$.

A center of symmetry exists at each point of the 16-fold positions. The unit cell contains 8 formula units or molecules of $MgAl_2O_4$. The oxygen parameter, u , equals $3/8$ for the idealized structure, but is 0.387 in the actual structure (Bacon, 1952)

Lattice Constant.

$a_0 = 8.0833 \text{ \AA}$ at 26°C (Swanson and Fuyat, 1953).

$= 8.06 \pm 0.005 \text{ \AA}$ for pure spinel (Roy et al., 1953).

$= 7.93 \text{ \AA}$ for limit of solid solution at 86 mol % Al_2O_3
(Roy et al., 1953).

X-ray Diffraction. Intensities, d-spacings, and indices of diffracting planes of spinel (from Swanson and Fuyat, 1953) are given on Card No. 5-0672, X-ray Powder Data File, American Society for Testing Materials.

Physical Constants

	<u>MgO·Al₂O₃</u>	<u>MgO·3.5 Al₂O₃</u>
<u>Melting Point.</u>	2135°C ¹	2030°-2060°C ²
<u>Density.</u>	3.6 g/cc ¹	3.61 g/cc ²
<u>Coefficient of Thermal Expansion.</u>	(in. in. ⁻¹ °C ⁻¹)	
100°C	6.6-8.5 x 10 ⁻⁶	³
25-800°C	7.6 x 10 ⁻⁶	⁴
100°-900°C	8.9 x 10 ⁻⁶	⁵
25°-1350°C	7.9 x 10 ⁻⁶	⁶
<u>Coefficient of Thermal Conductivity.</u>	(cal.sec. ⁻¹ C° ⁻¹ cm. ⁻² cm.)	
100°C	.0357	⁷
400°C	.0244	⁷
800°C	.0159	⁷
1200°C	.0130	⁷
<u>Specific Heat.</u>		
20°C	0.2	³
1040°C	0.214-0.257	⁸

¹Handbook of Chemistry and Physics (1962).

²Synthetic Crystal Data Sheet, Linde Air Products Co.

³Archibald and Smith (1953).

⁴Riecke and Blicke (1931).

⁵Rigby, et al. (1946).

⁶Anderson (1952).

⁷Kingery, et al. (1954).

⁸Salmang (1961).

Electrical Properties

Electrical Conductivity (polycrystalline spinel).

<u>Temperature °C</u>	<u>Conductivity in $\text{ohm}^{-1} \text{cm.}^{-1}$</u>		
	Jander and Stamm (1931)	Roegener (1940)	Bradburn and Rigby (1953)
435		2.0×10^{-8}	
520		1.5×10^{-7}	
700			1.58×10^{-7}
730		5.0×10^{-7}	
800			4.00×10^{-7}
835		1.0×10^{-6}	
900	1.19×10^{-6}		1.00×10^{-6}
925		2.0×10^{-6}	
940	1.78×10^{-6}		
975	2.38×10^{-6}		
985		4.5×10^{-6}	
1000	4.00×10^{-5}		5.00×10^{-5}
1035		5.0×10^{-6}	
1059	5.32×10^{-5}		

Dielectric Constant. 8 or 9 (Synthetic Crystal Data Sheet, Linde Air Products Co.).

Optical Properties

Index of Refraction. $1.727 (589.3 \text{ \AA } n_d)^1$
 $1.720-1.717$ (on commercial crystal)²
 1.708 (stoichiometric spinel)²

Chromatic Dispersion. $0.012 (n_F - n_C, 6563 \text{ to } 4861 \text{ \AA})^2$

$$= \frac{n_d^{-1}}{n_F - n_C} \approx 65^2$$

Infrared Transmission at $10,000 \text{ \AA}$. 85% (5 mm. thickness)²

Infrared Limit of Transparency. $53,000 \text{ \AA}$ (30% transmission)²

¹Synthetic Crystal Data Sheet, Linde Air Products Co.

²Wickersheim and Lefever (1960).

Mechanical Properties

Ultimate Strength in Compression.

Temperature	Sintered Spinel ¹	Hot Pressed Spinel ²
20°C	270,000 psi	390,000 psi
500	200,000	
800	170,000	
1100	140,000	
1200	71,000	
1400	21,000	
1500	8,500	

Ultimate Strength in Tension.

Temperature	Sintered Spinel ³
20°C	19,200
550	13,000
900	10,800
1600	6,100
1300	1,140

Outer Fiber Tensile Strength, Transverse Bending.

Temperature	Sintered Spinel ⁴	Hot Pressed Spinel ⁵
20°C	12,300 psi	33,400 psi
400	12,200	
600	11,900	
1000	10,900	
1200	9,500	
1300	7,900	

¹Ryschkewitsch (1941a).

²Palmour, H. and Choi, D. M.
unpublished work, 1962.

³Ryschkewitsch (1941b)

⁴Anderson (1952)

⁵Palmour, et al. (1962b)

Ultimate Strength in Torsional Shear.

Temperature	Sintered Spinel ¹
20°C	9,450 psi
800	8,150
1000	7,550
1200	6,550
1300	5,250

Torsional Creep Rate.

Temperature	Applied Stress	Sintered Spinel ¹
1100	1200 psi	$1.36 \times 10^{-6} \text{ in. in.}^{-1} \text{ hr.}^{-1}$
1200	1800	6.30×10^{-6}
1200	2400	9.25×10^{-6}
1300	1200	150×10^{-6}
1300	1800	263×10^{-6}

Young's Modulus of Elasticity.

Temperature	Sintered Spinel ¹	Hot Pressed Spinel ²
25°C	$34.5 \times 10^6 \text{ psi}$	$35 \times 10^6 \text{ psi}$
800	32.9×10^6	
1000	30.4×10^6	
1100	28.0×10^6	
1200	25.0×10^6	
1300	20.1×10^6	

¹Anderson (1952)

²Palmour et al. (1962b)

Rigidity Modulus, Poisson's Ratio.

Temperature	Sintered Spinel ¹	
	G	ν
25°C	13.2×10^6 psi	0.31
800°C	11.6×10^6	0.42
1000°C	10.3×10^6	0.47
1100°C	9.5×10^6	0.47
1200°C	8.5×10^6	0.47
1300°C	7.2×10^6	0.45

Hardness. 8 on Mohs' scale.

Microhardness. Polished sintered spinel, measured with a square diamond pyramid, gave values of 1000 kg/mm².² For variation of microhardness with crystallographic orientation see Section VII of this report.

¹Anderson (1952).

²Hill (1932).

APPENDIX B

ANALYTICAL PROCEDURES FOR DETERMINATION OF Mg^{++} AND Al^{+++} IN SPINEL

It is desirable to know the exact alumina-magnesia mole ratio both before and after the growth of spinel single crystals. This requires a complete dissolution of the sample followed by an accurate chemical analysis for aluminum and magnesium.

A number of methods for fusion were tried: the standard sodium carbonate, sodium bicarbonate, potassium bisulfate, potassium pyrosulfate and alkali hydroxide suggested by Hillebrand, *et al.* (1953) and the phosphoric acid + sulfuric acid mixture of Mendlina, *et al.* (1959). Potassium bisulfate was most nearly effective on spinel feed materials, but none were successful with crushed single crystal spinel specimens. Recently, a method which gives a complete fusion of both spinel feed materials and spinel single crystals has been devised. The sample is mixed with at least ten times its weight of reagent grade potassium fluoride in a platinum crucible and enough hydrofluoric acid is added to the crucible to completely cover the mixture. Then its contents are heated to dryness over a low Bunsen flame, taking particular care to avoid spattering. Thereafter, the crucible and its contents are placed in a furnace at about 500°C and maintained at this temperature for one-half hour. After cooling, the contents are washed into a polypropylene beaker with distilled water, and concentrated hydrochloric acid is added to this solution until it becomes clear.

It should be particularly noted that solutions containing fluoride ion and/or hydrofluoric acid in high concentrations attack glass, requiring the use of plastic laboratory ware in the procedures described here. In addition, the presence of fluoride causes difficulties with analyses carried out at high pH values, since it promotes the partial precipitation of magnesium fluoride during the determination. For these reasons, the possibility of distilling off hydrofluoric acid by adding sulfuric acid to the solution obtained from fusion and boiling is the subject of a current investigation.

While an effective method of fusion has been under investigation, a search also has been underway for a reliable method of separating aluminum from magnesium in solutions carrying known (large) amounts of reagent grade aluminum and magnesium salts.

Since aluminum precipitates as aluminum hydroxide between pH 3 and pH 12, it is more advantageous to carry out the aluminum analysis first. Eight-hydroxyquinoline and ammonium hydroxide precipitations were tried for aluminum

analysis (Kolthoff, et al., 1953). Both methods gave accurate and quite reproducible results. The filtrate left from aluminum precipitation was used to determine the amount of magnesium. For magnesium determination, both EDTA (disodium salt of ethylene diamine tetra-acetic acid) titration and pyrophosphate precipitation were used. The filtrates obtained from ammonium hydroxide precipitation for aluminum gave good and reproducible results for magnesium with both EDTA titration (Schwarzenbach, 1955) and pyrophosphate precipitation (Kolthoff, et al., 1953). The filtrates obtained from eight-hydroxyquinoline precipitation of aluminum gave accurate and reproducible results when analyzed for magnesium by using pyrophosphate precipitation. However, EDTA titration did not give good results for magnesium in the filtrates left from eight-hydroxyquinoline precipitation. Consequently, filtrates containing eight-hydroxyquinoline were heated to dryness to drive off eight-hydroxyquinoline, but the magnesium content determined by EDTA titration was low.

APPENDIX C

SLIP CASTING OF SPINEL AND ALUMINA CRUCIBLES

A technique for slip casting small alumina crucibles ($2\frac{1}{8}$ in. high by 1 in. diameter at top) and their lids has been in use for several years at this laboratory. The slip is prepared by milling Alcoa A-14 alumina with 45% water and 1.5% Darvan No. 7¹ for 48 hours in a McDanel 96% Al_2O_3 jar mill. Casting requires about 3 minutes in Puritan pottery plaster molds, with release occurring in about 15-20 minutes. The well-dried cast pieces are fired to about 1850°C for 30 minutes in a small oxy-acetylene fueled furnace.

Spinel crucibles of the same small size were successfully slip cast using this technique without any particular difficulty, and sintered at 1850°C to approximately 98% theoretical density. However, the much larger spinel crucibles needed as non-contaminating containers in which high purity spinel feed materials could be calcined in substantial quantity were cast only after making several changes in the basic procedure. The modified technique, while partially successful (useful crucibles were produced, but with considerable difficulty), was not considered fully reproducible because of variations in raw materials, particle sizes, and aging effects in the prepared slip. Perhaps the most serious problem was the extreme fragility of the relatively thin-walled cast piece, 6 in. diameter by $8\frac{1}{8}$ in. high prior to firing.

Furthermore, the large quantities of slip required for casting such a shape required the production of multiple batches of spinel (by calcination of alumina and basic magnesium carbonate in a gas-fired furnace to 1450°C). Because of the high costs of producing this material without suitable calcining crucibles, and the lack of control of slip made from such multiple lots, additional slip casting experiments to improve the processing of large crucibles were carried out with commercially available alumina, since techniques appropriate for large alumina crucibles should prove to be readily transferable to spinel as well.

After considerable experimentation, satisfactory alumina crucibles ($5\frac{1}{8}$ in. diameter by $7\frac{1}{2}$ in high after firing) were produced by the

¹Darvan No. 7, a polyelectrolyte deflocculent, is a product of the R. T. Vanderbilt Company, New York, N. Y.

following method:

1. The slip was prepared using 30% water and 1% Darvan based on the dry weight of the Alcoa A-14 alumina used in the batch. Magnesium fluoride (0.25 weight percent) was also added to facilitate grain size control and improved firing behavior of the alumina body.
2. Milling was done under optimum conditions (1.5 kg. of alumina, 4 kg grinding media, 25% water) for 24 hours in a one gallon capacity McDanel 96% alumina jar mill.
3. After milling, 1/4% PVA (polyvinyl alcohol) in solution was added to the slip, bringing the total water content up to 30% (based on dry weight of alumina used). The small amount of froth formed by mixing the PVA solution with the slip was easily removed by adding a few drops of octyl alcohol-ether solution to the slip.
4. The slip was poured into plaster molds and allowed to cast five minutes to obtain a 1/4 inch wall thickness.² The draining of the mold was very critical, requiring a smooth, uniform motion to avoid erosion of the casting.
5. The cast pieces were allowed to air-dry in the mold for 24 hours, then they were carefully dried in a controlled humidity drier (100°F dry bulb, 95°F wet bulb initial conditions) over a period of 3 to 4 days.
6. The dry crucibles were fired to 1700-1750°C in a gas fired furnace in about seven hours yielding good, well matured crucibles 7-1/2 inches high by 5-1/8" outside diameter. Some "sagger drag" and distortion of the lids, which served as setters for the inverted crucibles, was attributed to the rapidity of firing in this manually controlled furnace.

At present, the alumina crucibles described above are being employed without evidence of difficulty at temperatures up to 1450°C for calcination of spinel materials required in other phases of the program. In the future, the improved casting techniques developed for the large alumina crucibles will be brought to bear again on the matter of spinel crucibles for use where extreme purity during calcination is indicated.

²(The molds had been formed on smooth-surfaced metal mandrels, using 65% water-plaster slurry based on dry weight of the Puritan pottery plaster).

APPENDIX D

MATERIAL ANALYSES

Chemical Analyses of Raw Materials

Basic Magnesium Carbonate, U. S. P. Grade.

The Phillip Carey Manufacturing Company
Plymouth Meeting, Pa.

Chemical formula: $3 \text{MgCO}_3 \cdot \text{Mg}(\text{OH})_2 \cdot 3\text{H}_2\text{O}$

<u>Component</u>	<u>Weight Percent</u> *
Magnesium Oxide (MgO)	42.3
Iron (Fe)	0.015
Calcium Oxide (CaO)	0.50
Chlorides (Cl)	Nil
Moisture	1.50
Soluble salts	0.20

Alumina, Alcoa A-14 Grade.

Aluminum Company of America
Pittsburgh 19, Pa.

Chemical Formula: Al_2O_3

<u>Component</u>	<u>Weight Percent</u> *
Al_2O_3	99.6
SiO_2	0.12
Fe_2O_3	0.03
Na_2O	0.04
Loss of Ignition (1100°C)	0.2
Total H_2O (by Sorption-Ignition Test)	0.3

*Manufacturer's typical analysis.

Semiquantitative Spectrographic Analyses of Feed Materials
for Crystal Growth¹

<u>Impurity</u>	<u>Approximate impurity content in parts per million</u>		
	<u>Linde Spinel Boule Powder²</u>	<u>N. C. State Stoichiometric Spinel³</u>	<u>Linde Sapphire Boule Powder⁴</u>
Fe	100	500	10
B	50	100	500
Si	50	1000	1000
Pb	1000	500	500
Mo		50	
Ti	100	50	
Ca	50	500	10
Cu	1	5	
Cr		10	
Ba	10	500	10
Mg			500

¹Analyses by Dr. G. G. Long, Chemistry Dept., N. C. State College.

²AP333 Spinel Boule Powder, a product of Linde Air Products Co.,
A Division of Union Carbide Corp., New York, N. Y.

³Prepared by calcination at 1450°C of equal molar ratios of Linde's
alumina boule powder and basic magnesium carbonate (see Section IV, p. 18).

⁴A product of Linde Air Products Company, A Division of Union Carbide
Corp., New York, N. Y.

LIST OF REFERENCES

- Alper, A. M., McNally, R. M., Ribbe, P. H. and Doman, R. C. 1962.
The System $\text{MgO-MgAl}_2\text{O}_4$. J. Am. Ceram. Soc. 45 (6) 263-68
- Anderson, H. H. 1952. Magnesium Aluminate Spinel as a Refractory Material.
Unpublished Ph.D. Thesis, Massachusetts Institute of Technology, Cambridge.
- Archibald, W. A. and Smith, E. J. D. 1953. Super-Refractories. Ceramics:
A Symposium, (A. T. Green and G. H. Stewart, Ed.) 536-591. The British
Ceramic Society, London.
- Bacon, G. E. 1952. A neutron-diffraction study of magnesium-aluminum oxide.
Acta. Crystallogr. 5 684-686.
- Barth, T. W. and Posnjak, E. 1932. Spinel structures: with and without variate
atom equipoints. Z. Krist. 82 325.
- Bauer, W. E., Gordon, I. and Moore, C. H. 1950. Flame fusion synthesis of
mullite single crystals. J. Am. Ceram. Soc. 33 (4) 140-143.
- Beevers, C. A. and Ross, M. A. S. 1937. The crystal structure of "Beta Alumina,"
 $\text{Na}_2\text{O} \cdot 11\text{Al}_2\text{O}_3$. Z. Krist. 97 59.
- Bradburn, T. E. and Rigby, G. R. 1953. Electrical Conductivity of Spinel.
Trans. Brit. Ceram. Soc. 52 (3) 417-35.
- Brugg, W. H. 1915. The structure of the spinel group of crystals. Phil. Mag.
30 305.
- Brun, E., Hafner, S., Hartman, P. and Laves, F. 1960. Elektrische
Quadrupolwechselwirkung von Al^{27} und Kationverteilung in Spinell (MgAl_2O_4).
Naturwissenschaften 47 (12) 277.
- Carter, R. E. 1961. Mechanism of solid-state reaction between magnesium oxide
and aluminum oxide and between magnesium oxide and ferric oxide.
J. Am. Ceram. Soc. 44 (3) 116-20.
- Chalmers, B. 1955. Effects of impurities and imperfections on crystal growth.
Impurities and Imperfections. (O. T. Markze, Ed.) 84-106.
American Society for Metals, Cleveland, Ohio.
- Choi, D. M., McBrayer, R. D. and Palmour, H. III. 1961. Effects of irradiation
upon the microindentation behavior of sapphire. Presented at the 63rd
annual meeting of the American Ceramic Society, Toronto. Being submitted
for publication.

- Clark, G. L., Howe, E. E. and Badger, A. E. 1934. Lattice dimensions of some solid solutions in the system $\text{MgO}-\text{Al}_2\text{O}_3$. J. Am. Ceram. Soc. 17 (1) 7-8.
- Czochralski, J. 1917. Measuring the velocity of crystallization of metals. Z. Physik. Chem. 92 219-21.
- De La Rue, R. E. and Halden, F. A. 1960. Arc-image furnace for growth of single crystals. Rev. Sci. Instr. 31 (1) 35-38.
- Eppler, W. F. 1943. Über das Harten synthetischer Spinelle. Z. Angew. Mineral. 4 345-362.
- Evans, R. C. 1952. An Introduction to Crystal Chemistry. 171. Cambridge University Press, Cambridge.
- Ewald, P. P. and Herman, C. 1926. Strukturberichte 1913-1926. 350.
- Field, W. G. 1961. Modern single crystal technology. Presented in Fall Meeting, Basic Science Division, The American Ceramic Society, Schenectady, N. Y. September 1961 (1-B-61 F).
- Field, W. G. and Bauer, W. H. "Plasma techniques for the growth of single crystals." Presented at Fall Meeting, Basic Science Division, The American Ceramic Society, Schenectady, N. Y. September 1961 (24B-61F).
- Fisher, W. A. and Hoffman, A. 1954. Volumenänderungen in der Diffusionszone von Oxidsystemen. Naturwissenschaften. 41 162.
- Frank, C. 1952. Advances in physics. Phil. Mag. Supplement 1. 1.
- Fuerstenau, D. W., Fulrath, R. H. and Pask, J. A. 1961 and 1962. A fundamental study of the variables associated with the mixing of ceramic raw materials. Inst. of Engr. Research, University of California. Quarterly Progress Reports Nos. 2, 4 and 5. Contract No. AF33(616)-7763. Wright Air Development Division.
- Handbook of Chemistry and Physics. 1962. (C. D. Hodgman, R. C. Weast and S. M. Selby, Ed.) 43rd Edition, p. 340. Chemical Rubber Publishing Co., Cleveland, Ohio.
- Hild, K. 1932. Die Bildung des Spinells Al_2ZnO_4 durch Reaktion in festen Zustand. Z. Physik. Chem. A. 161 305.
- Hillebrand, W. F., Lundell, G. E., Bright, H. A. and Hoffman, J. I. Applied Inorganic Analysis. 2nd Edition. John Wiley and Sons, Inc., New York. 336-343.

- Hornstra, J. 1960. Dislocations, stacking faults, and twins in the spinel structure. J. Phys. Chem. Solids. 15 311-323.
- Hornstra, J. 1962. Dislocations in spinels and related structures. Chapter 4. Structure and Properties of Engineering Materials. Plenum Press, New York (In Press).
- Iida, S. 1957. Layer structures of magnetic oxides. J. Phys. Soc., Japan. 12 222.
- International Tables of X-ray Crystallography. 1952. (N. F. M. Henry and K. Lonsdale, Ed.). Vol. I. 340. Kynoch Press, Birmingham, England.
- Jagodzinski, H. 1957. Die Bestimmung einer bei der Entmischung Al_2O_3 - übersättiger Mg-Al-spinelle auftretenden Zwischenstruktur. Z. Kristallogr. 109 300-409.
- Jagodzinski, H. and Saalfeld, H. 1958. Kationenverteilung und Strukturbeziehungen in Mg-Al-Spinellen. Z. Kristallogr. 110 197.
- Jander, W. and Stamm, W. 1931. Der innere Aufbau fester anorganischer Verbindungen bei höheren Temperaturen. Z. anorg. u. allgem. Chem. 199 165.
- Kingery, W. D., Franch, J., Coble, R. L. and Vasilos, T. 1954. Thermal conductivity: X, data for several pure oxide materials corrected to zero porosity. J. Am. Ceram. Soc. 37 107-110.
- Knoop, F., Peters, C. G. and Emerson, W. F. 1939. A sensitive pyramidal-diamond tool for indentation measurements. J. Research Nat. Bur. Standards. 23 R. P. 1220. 39-61.
- Kolthoff, I. M. and Sandell, E. B. 1953. Textbook of Quantitative Inorganic Analysis. 3rd Edition. The MacMillan Company, New York. 318-321, 352-363.
- Kronberg, L. L. 1960. Deformation of Refractory Crystals. Semi-Annual Report No. 1 (Sept., 1960). Contract No. AF-33(616)-5511. General Electric Research Laboratory, Schenectady, N. Y.
- Laudise, R. A. and Ballman, A. A. 1958. Hydrothermal synthesis of sapphire. J. Am. Chem. Soc. 80 (11) 2655-57.
- Lefever, R. A. and Clark, G. W. 1962. Multiple-tube flame fusion burner for the growth of oxide single crystals. Rev. Sci. Instrs. 33 (7) 769-770.
- Levy, P. W. 1961. Annealing of the defects and color centers in unirradiated and in reactor irradiated Al_2O_3 . Presented at the Faraday Society Meeting at Seclay, France, April, 1961.

- Linder, R. 1955. Formation of spinels and silicates by reactions in the solid state, investigated by method of radioactive tracers. Z. Electrochem. 59 (10) 967-970.
- Linder, R. and Åkerström, A. 1956. Self-diffusion and reaction in oxide and spinel systems. Z. physik. Chem., Neue Folge 6 162-177.
- Nachatschi, F. 1932. Der Magnesium-Gallium-Spinell. Z. Krist. 82 343.
- Ngan, A. and Forestier, H. 1956. Sur le durcissement par revenu d'une solution solide, sursaturée, trempée, d'alumine dans le spinelle de magnésium. Compt. Rend. 242 (2) 1893-1895.
- McBrayer, R. D. 1962. Effect of atmosphere upon a precipitation hardening phenomenon in alumina-rich spinel. Unpublished M. S. Thesis, North Carolina State College, Raleigh.
- Mendlina, N. G., Novoselova, A. A. and Rychkov, R. S. 1959. Dissolution of fused aluminum oxide and the determination of impurities. Zavod. Lab. (Moscow) 25 (11) 1293-1294; Anal. Abstr. 7, art. 3163. 1960.
- Navias, L. 1961. Preparation and properties of spinel made by vapor transport and diffusion in the system $MgO-Al_2O_3$. J. Am. Ceram. Soc. 44 (9) 434-446.
- Navias, L. 1962. Development of magnesium aluminate spinel by vapor transport and diffusion in vacuo and in medium gas pressures. Report No. 62-RL-2943M. General Electric Co., Schenectady, N. Y.
- Nishikawa, S. 1915. The structure of some crystals of the spinel group. Proc. Tokyo math.-phys. Soc. 8 199.
- Palmour, H. III, Choi, D. M., Barnes, L. D., McBrayer, R. D. and Kriegel, W. W. 1962a. Deformation in hot pressed polycrystalline spinel. Contract DA-01-009-ORD-903. Technical Report No. 1. North Carolina State College, Raleigh.
- Palmour, H. III, Choi, D. M. and Kriegel, W. W. 1962b. Relationships between mechanical strength and microstructure in hot pressed $MgAl_2O_4$ spinel. Presented at 64th Annual Meeting of the American Ceramic Society. To be submitted for publication.
- Palmour, Hayne III and Kriegel, W. W. 1961. The influence of diffused transition metal oxides on the micromechanical properties of single crystal sapphire. Presented at the Basic Science Div., Am. Ceram. Soc., Sept., 1961. To be submitted for publication.

- Popov, S. K. 1959. Growing Synthetic Corundum as Rods and Boules Growth of Crystals. (Shubnikov, A. V., Ed.) Vol. 2, Translated from the Russian by Consultant's Bureau, Inc., New York.
- Rankin, G. A. and Merwin, H. E. 1916. The ternary system $\text{CaO-MgO-Al}_2\text{O}_3$. J. Am. Chem. Soc., 38 571.
- Reed, Thomas B. 1961(a). Induction-coupled plasma torch. J. Appl. Phys. 32 821.
- Reed, Thomas B. 1961(b). Growth of refractory crystals using the induction plasma torch. J. Appl. Phys. 32 2534.
- Reed, Thomas B. 1962. Plasma torches. Internat. Sci. and Tech. 1 (6) 42-48, 76.
- Riecke, R. and Blicke, K. 1931. "Über Herstellung, Eigenschaften und technische Verwendung einiger Spinelle. Ber. deut. Keram. Ges. 12 163.
- Rigby, G. R. 1953. The spinels and their relation to chrome ores. Ceramics: A Symposium. (A. T. Green and G. H. Stewart, Ed.) 488-512. The British Ceramic Society, London.
- Rigby, G. R., Lovell, G. H. B. and Green, A. T. 1946. Some properties of the spinels associated with chrome ores. Trans. Brit. Ceram. Soc. 45 137.
- Rinne, F. 1928. Morphologische und physikalisch-chemische Untersuchungen an synthetischen Spinellen als Beispielen unstoichiometrisch zusammengesetzter Stoffe. N. Jb. Mineral (A) Beil. - Bd. 58 431-108.
- Roegener, H. 1940. "Über den Gleichstromwiderstand keramischer Werkstoffe. Z. Elektrochem. 46 25.
- Roy, D. M., Roy, R. and Osborn, E. F. 1953. The system $\text{MgO-Al}_2\text{O}_3\text{-SiO}_2$ and influence of carbonate and nitrate ions on the phase equilibria. Am. J. Sci. 251 (5) 337-61.
- Rudness, R. G. and Kebler, R. W. 1960. Growth of single crystals of incongruently melting yttrium-iron garnet by flame fusion process. J. Am. Ceram Soc. 43 (1) 17-22 (1960)
- Ryschkewitsch, E. 1941a. "Über die Druckfestigkeit einiger keramischer Werkstoffe auf der Einstoff-Basis. Ber. deut. Keram. Ges. 22 (2) 54-65.
- Ryschkewitsch, E. 1941b. "Über die Zerreißfestigkeit einiger keramischer Werkstoffe auf der Einstoff-Basis. Ber. Deut. Keram. Ges. 22 363-371.

- Ryshkewitch, E. 1960. Oxide Ceramics: Physical Chemistry and Technology. Academic Press, New York.
- Saalfeld, H. and Jagodzinski, H. 1957. Die Entmischung Al_2O_3 - "übersättigter" Mg-Al-Spinelle. Z. Kristall. 109 (2) 87-109.
- Salmang, H. 1961. Ceramics: Physical and Chemical Fundamentals (translated by Marcus Francis). Butterworths, London.
- Schwarzenbach, G. 1955. Die Komplexometrische Titration. Interscience Publisher, New York.
- Sheuplein, R. J. and Gibbs, P. 1960. Surface structure in corundum: I. Etching of dislocations. J. Am. Ceram. Soc. 43 (9) 458-72.
- Stewart, M. T., Thomas, R., Wauchope, K., Winegard, W. C. and Chalmers, B. 1951. New segregation phenomenon in metals. Phys. Rev. 83 (2) 657.
- Stocker, J. and Collongues, R. 1957. Sur la préparation de composés réfractaires à base de zircone par la méthode de précipitation à l'état amorphe. Comptes Rendus. 245 431.
- Swanson, H. E. and Fuyat, R. K. 1953. Standard X-ray diffraction powder patterns. Nat. Bur. Stand. Circular. 539. Vol. II 35-38.
- Verma, A. R. 1953. Crystal Growth and Dislocations. Butterworth Scientific Publications, London.
- Verneuil, A. 1902. Production artificielle du rubis par fusion. Compt. Rend. 135 791-94.
- Wagner, C. 1946. The mechanism of formation of ionic compounds of higher order. (Double salts, spinels, silicates). Z. Physik. Chem. B34 309-316.
- Wickersheim, K. A. and Lefever, R. A. 1960. Optical properties of synthetic spinel. J. Opt. Soc. Am. 50 (8) 831-32.